Since January 2020 Elsevier has created a COVID-19 resource centre with free information in English and Mandarin on the novel coronavirus COVID-19. The COVID-19 resource centre is hosted on Elsevier Connect, the company's public news and information website.

Advanced Drug Delivery Reviews 179 (2021) 113998

Contents lists available at ScienceDirect

Advanced Drug Delivery Reviews

journal homepage: www.elsevier.com/locate/adr

Ultrasonic particles: An approach for targeted gene delivery

Aidan P.G. Walsh [a,b,c,1], Henry N. Gordon [a,b,d,1], Karlheinz Peter [b,c,e,f], Xiaowei Wang [a,b,c,e,f,*]

[a] Molecular Imaging and Theranostics Laboratory, Baker Heart and Diabetes Institute, Melbourne, VIC, Australia
[b] Atherothrombosis and Vascular Biology Laboratory, Baker Heart and Diabetes Institute, Melbourne, VIC, Australia
[c] Department of Medicine, Monash University, Melbourne, VIC, Australia
[d] Department of Biochemistry and Pharmacology, University of Melbourne, VIC, Australia
[e] Department of Cardiometabolic Health, University of Melbourne, VIC, Australia
[f] La Trobe Institute for Molecular Science, La Trobe University, Melbourne, VIC, Australia

ARTICLE INFO

Article history:
Received 30 June 2021
Revised 24 September 2021
Accepted 5 October 2021
Available online 15 October 2021

Keywords:
Gene transfer
Microbubble
Nucleic acid
Sonoporation
Targeted therapy
Ultrasonic irradiation

ABSTRACT

Gene therapy has been widely investigated for the treatment of genetic, acquired, and infectious diseases. Pioneering work utilized viral vectors; however, these are suspected of causing serious adverse events, resulting in the termination of several clinical trials. Non-viral vectors, such as lipid nanoparticles, have attracted significant interest, mainly due to their successful use in vaccines in the current COVID-19 pandemic. Although they allow safe delivery, they come with the disadvantage of off-target delivery. The application of ultrasound to ultrasound-sensitive particles allows for a direct, site-specific transfer of genetic materials into the organ/site of interest. This process, termed ultrasound-targeted gene delivery (UTGD), also increases cell membrane permeability and enhances gene uptake. This review focuses on the advances in ultrasound and the development of ultrasonic particles for UTGD across a range of diseases. Furthermore, we discuss the limitations and future perspectives of UTGD.

Contents

Abbreviations: AAA, abdominal aortic aneurysm; AKT, protein kinase B; BDNF, brain-derived neurotrophic factor; BNT162b2, BioNTech COVID-19 mRNA vaccine; C_3F_8, octafluoropropane; C_4F_{10}, decafluorobutane; CD105, endoglin, cluster of differentiation 105; COVID-19, coronavirus disease 2019; CVD, cardiovascular disease; DC-CHOL, DC-cholesterol; DNA, deoxyribonucleic acid; DOTAP, 1,2-dioleoyl-3-trimethylammonium propane; DPPC, dipalmitoylphosphatidylcholine; DSPC, distearoylphosphatidylcholine; DSPC-PEG2K-Mal, distearoylphosphatidylcholine-N-[*maleimide*(polyethylene glycol)-2000]; DSPE, 1,2-distearoyl-*sn*-glycero-3-phosphorylethanolamine; DSPE-PEG2000, 1,2-distearoyl-*sn*-glycero-3-phosphoethanolamine-N-[polyethylene glycol-2000]; DSTAP, 1,2-distearoyl-3-trimethylammonium-propane; eGFP, enhanced green fluorescence protein; GDNF, glial cell line–derived neurotrophic factor; GFP, green fluorescence protein; IFN-β, interferon-β; I/R, ischemia/reperfusion; LNP, lipid nanoparticle; MAdCAM-1, mucosal addressin cell adhesion molecule 1; Man-PEG2000, mannose-binding polyethylene glycol-2000; MB, microbubble; MI, myocardial infarction; miRNA, microRNA; MMP2, matrix metallopeptidase-2; MRI, magnetic resonance imaging; mRNA, messenger RNA; mRNA1273, Moderna COVID-19 mRNA vaccine; NB, nanobubble; Nurr1, orphan nuclear receptor; OTC, ornithine transcarbamylase; pDNA, plasmid DNA; PEG, polyethylene glycol; PEGylated-PEI-SH, polyethylene glycol-polyethylenimine-thiol; PEI, polyethylenimine; PMO, phosphorodiamidate morpholino oligomer; PNA, peptide nucleic acid; RNA, ribonucleic acid; SARS-CoV-2, severe acute respiratory syndrome coronavirus 2; SCF, stem cell factor; SF_6, sulfur hexafluoride; shRNA, short hairpin RNA; siRNA, small interfering RNA; SPIO-NP, fluorinated iron oxide nanoparticle; TA, tibialis anterior; Timp3, tissue inhibitor of metalloproteinase 3; TUNEL, terminal deoxynucleotidyl transferase dUTP nick end labeling; UTGD, ultrasound-targeted gene delivery; VCAM-1, vascular cell adhesion molecule-1; VEGF, vascular endothelial growth factor.

* Corresponding author at: Baker Heart and Diabetes Institute, 75 Commercial Road, Melbourne, VIC 3004, Australia.
E-mail address: xiaowei.wang@baker.edu.au (X. Wang).

[1] Equally contributing first authors.

https://doi.org/10.1016/j.addr.2021.113998
0169-409X/

1. Introduction

Gene therapy is the introduction of genetic materials into cells to compensate for an abnormal gene or allow the cells to produce beneficial proteins. The potential benefits of gene therapy have attracted major enthusiasm and consequently various gene therapy approaches have been investigated in relation to the treatment of genetic, acquired, and infectious diseases. Gene therapy has traditionally employed viral vectors to correct genetic abnormalities which result in clinical disorders. One of the most successful applications of gene therapy so far has been achieved in patients with severe combined immune deficiency or "bubble boy disease" [1,2]. However, while effective in treating genetic disorders, treatments using viral vectors have been associated with serious adverse events and the development of cancer, so several clinical trials have been stopped [3,4]. Subsequently, non-viral vectors have been proposed as alternatives with the promises of high transfection efficacy and increased gene expression without safety concerns. The current COVID-19 pandemic has supercharged innovation in gene therapy, resulting in the use of messenger RNA (mRNA) as a vaccine for severe acute respiratory syndrome coronavirus 2 (SARS-CoV-2) [5-8]. The use of lipid nanoparticles (LNPs) for the delivery of nucleic acids has several advantages. These include protection of the genetic materials from degradation, prevention of rapid systemic removal, and facilitation of cellular uptake. Comparing LNPs to the conventional viral vectors, the latter have been associated with carcinogenicity or immunogenicity, difficulty in production, and limitations in packaging capacity; therefore LNPs provide safer and more efficient delivery [9-15]. LNPs have been the platform for several genetic therapy systems, including the first Food and Drug Administration–approved small interfering RNA (siRNA) therapeutic, Onpattro®, for the treatment of hereditary transthyretin-mediated amyloidosis [16]. LNP platforms are also employed for the delivery of mRNA in the BNT162b2 and mRNA-1273 vaccines for SARS-CoV-2 [5-8,17]. However, most LNPs are delivered via intramuscular or intravenous injection. This is not site-specific for organs or cell types, resulting in off-target delivery. Therefore, LNPs have been further modified to achieve site-specific targeted gene delivery by responding to biological stimuli (pH or enzymes) or being triggered via the incorporation of external stimuli (light or ultrasound) [18]. In this review, we focus on the use of ultrasound and ultrasonic particles for targeted delivery of genetic materials across a range of diseases.

2. Ultrasound imaging

Among the clinical imaging modalities available, ultrasound imaging is the most widely used as this technology offers significant advantages. Ultrasound is safer for patients, as compared to X-ray or nuclear imaging, because it does not involve ionizing radiation. Therefore, the technology is well suited to routine clinical applications where frequent imaging is needed, such as screening and early disease detection. While most imaging modalities, such as magnetic resonance imaging (MRI) and positron emission tomography imaging, require large machines and complex housings, ultrasound scanners are light and highly portable. Over the last two decades, hand-held ultrasound units and laptop systems have become increasingly affordable and gained use in bedside applications, ambulances, and general practitioners' and other doctors' clinics. These point-of-care ultrasound scanners are particularly attractive for diagnostic imaging in rural areas and developing countries. More importantly, ultrasound procedures provide inherent real-time imaging and can be completed within minutes. Ultimately, there are no known long-term side effects of ultrasound imaging, while the procedure is painless and rarely causes any discomfort.

2.1. Clinical use of ultrasound

The most common clinical use of diagnostic ultrasound is for obstetric imaging of growth and fetal development during pregnancy. Other common uses include imaging of the abdomen, brain, blood vessels, eyes, glands, heart, muscles, and skin. It is also used for ultrasound-guided procedures such as during tissue collection for biopsies and during needle placement. Another clinical use of ultrasound is high-intensity focused therapeutic ultrasound, where increased levels of acoustic power are focused on specific targets. Further, therapeutic ultrasound is used for pain reduction and improvement in the circulation and mobility of soft tissue, as well as in the treatment of many cancers, such as bone tumors, breast, kidney, and liver cancers, and pancreatic and uterine fibroids.

2.2. Advances in ultrasound technology

Ultrasound imaging has undergone dramatic advances over the last few decades and its use as a diagnostic imaging modality has continued to evolve. While initially ultrasound imaging started

with brightness-mode systems that produced poor, bi-stable images, it has now progressed to portable hand-held devices that are capable of high-resolution real-time grey-scale imaging, tissue harmonic evaluation, and color-flow Doppler. Improvements in acquisition and analysis of contrast enhancement, motion-derived indices, shear wave elastography, strain, and speckle tracking have added further details for better diagnostic assessment [19-22]. Ultrasound is known to be operator dependent, so many groups have researched artificial intelligence–powered ultrasound to overcome this limitation [23,24].

Conventional diagnostic ultrasound imaging has a high temporal resolution and its spatial resolution can be improved and sharper images obtained by using higher frequency ultrasound waves. A higher frequency of ultrasound results in a shorter wavelength and therefore a shallower depth of penetration [25]. Increased frequency, however, allows the tissues to absorb the energy more readily, therefore producing images that are more faint. At 3.5 MHz imaging depth of 10–20 cm is possible, while at 50 MHz the depth is limited to<1 cm [26]. Clinically, high-frequency ultrasound is most useful in areas such as skin imaging and imaging during minimally invasive surgery where resolution is critical but penetration requirements are small [26]. However, high-frequency ultrasound is also a valuable tool for preclinical imaging, in particular the imaging of small animals such as mice and zebrafish [27-31], unlocking many opportunities for drug and gene therapy research (Fig. 1).

3. Ultrasound contrast agents and ultrasonic particles

The sound-scattered signal from blood is similar to that from tissue; therefore, measurement of blood perfusion with ultrasound is difficult [32]. This challenge can now be overcome by the use of ultrasound contrast agents, also known as microbubbles (MBs). These agents were introduced to human ultrasound in 1968 by Gramaik and Shah, who observed that the reflection of ultrasound in the aortic root after injection of little air bubbles was noticeably enhanced [32,33]. MBs have a different density and compressibility to those of the blood and surrounding tissue [34]; therefore, when administrated in the blood pool or a cavity, they provide efficient backscattering of sound waves which results in enhancement of ultrasonic signals [35]. Ultrasound contrast agents are administered into the venous system, where they are rapidly distributed by blood flow to the imaging site, and the contrast enhancement is typically apparent within seconds [32]. These agents include MBs, echogenic liposomes, and perfluorocarbon droplets [34]. These highly compressible objects can resonate in the sound field, producing a non-linear acoustic response that enables detection strategies to differentiate between the echoes from the ultrasound contrast agent and those of the blood or tissue [34-40].

3.1. Development and use of ultrasound contrast agents

The properties of MBs are the result of both the material used for their shell and their gas core. Initially, these contrast-enhancing agents started with normal saline, which was agitated. Such bubbles had extremely limited storage stability and hence had to be prepared in the immediate vicinity of the patient [41]. The generation of these crude MBs was achieved through the agitation of blood and saline; consequently they lacked a shell and their gas core was simply air. Since these air-filled microspheres had high solubility in blood and were rapidly cleared by the lungs, they could only be visualized for a few seconds after intravenous administration. They were therefore not ideal for opacification of the left heart [42].

Subsequent improvements to the formulation of MBs have increased their stability and functionality. A thin shell comprising albumin or galactose palmitic acid enables the MBs to pass through the pulmonary capillary bed; however, they are incapable of recirculation in the bloodstream because they cannot resist arterial pressure gradients [36]. A thick shell provides stability but impairs their ability to resonate, causing a weak acoustic backscatter response [36]. Currently, the MB shell, designed to enhance *in vivo* stability, can be made of proteins, lipids, or biopolymers [43], with shell thickness varying from 10 to 200 nm [32]. Many lipid-shelled agents have polyethylene glycol (PEG) incorporated into the shell to enhance stability and reduce immune-system recognition [32]. More importantly, second-generation MBs are produced using water-insoluble gases such as perfluorocarbon octafluoropropane [C_3F_8], decafluorobutane [C_4F_{10}], and sulfur hexafluoride [SF_6] in order to prevent gas diffusion, which improves their survival and stability under pressure [32,43].

3.2. Clinical use of ultrasound contrast agents

Several MBs have been approved for clinical use, mainly for applications such as perfusion imaging, characterization of liver lesions, and blood pool enhancement [43]. Optison™ (GE Healthcare) is generated by sonication of human albumin with octafluoropropane, a perfluorocarbon gas. Lumason (Bracco) is a contrast agent stabilized with a lipid shell and filled with SF_6. The MBs are reconstituted by mixing saline with lyophilisate and are stable in the vial for approximately 6 h at room temperature after reconstitution. Sonazoid™ (GE Healthcare) are lyophilised MBs that encapsulate C_4F_{10} in a lipid membrane. Once it has been reconstituted, Sonazoid ™ should be used within 2 h. A similar product is Definity® (Lantheus Medical Imaging), a lipid shell with C_3F_8 gas, which has been shown to be stable for 12 h post activation of the vial. The current clinical indications for the administration of MBs are for patients who produce technically limited, suboptimal echocardiograms. For cardiac imaging, MBs are employed to improve visualization of the endocardia, enable assessment of the left ventricular structure/function, confirm or exclude echocardiographic diagnosis of left ventricular structural abnormalities, and assist in the detection and classification of intracardiac masses [44,45].

3.3. Preclinical use of ultrasound contrast agents and ultrasonic particles

In addition to anatomical imaging, advancement of micro-/nano-particles via material selection and technological development in ultrasound imaging has extended their functions for molecular imaging in preclinical settings [27,28]. By conjugating these contrast agents to ligands that target biomarkers, they can be used for direct visualization of diseases [46]. Furthermore, developments in biosensing of micro-/nano-bubbles have allowed for ultrasound imaging of reactive oxygen species production [47] and detection of pH changes *in vivo* [48]. Recent advances in nanotechnology and material sciences have led to the use of MBs as drug carriers for targeted drug and gene delivery [29,49,50].

4. Acoustic pressure and ultrasonic particles

By altering the acoustic pressure, the properties of these ultrasonic particles can be fine-tuned [51]. A low acoustic pressure will result in stable oscillation of ultrasonic particles, known as stable cavitation (Fig. 2).

Alternatively, a higher acoustic power setting will lead to the bursting or destruction of the MBs (Fig. 3) [52]. Both stable and

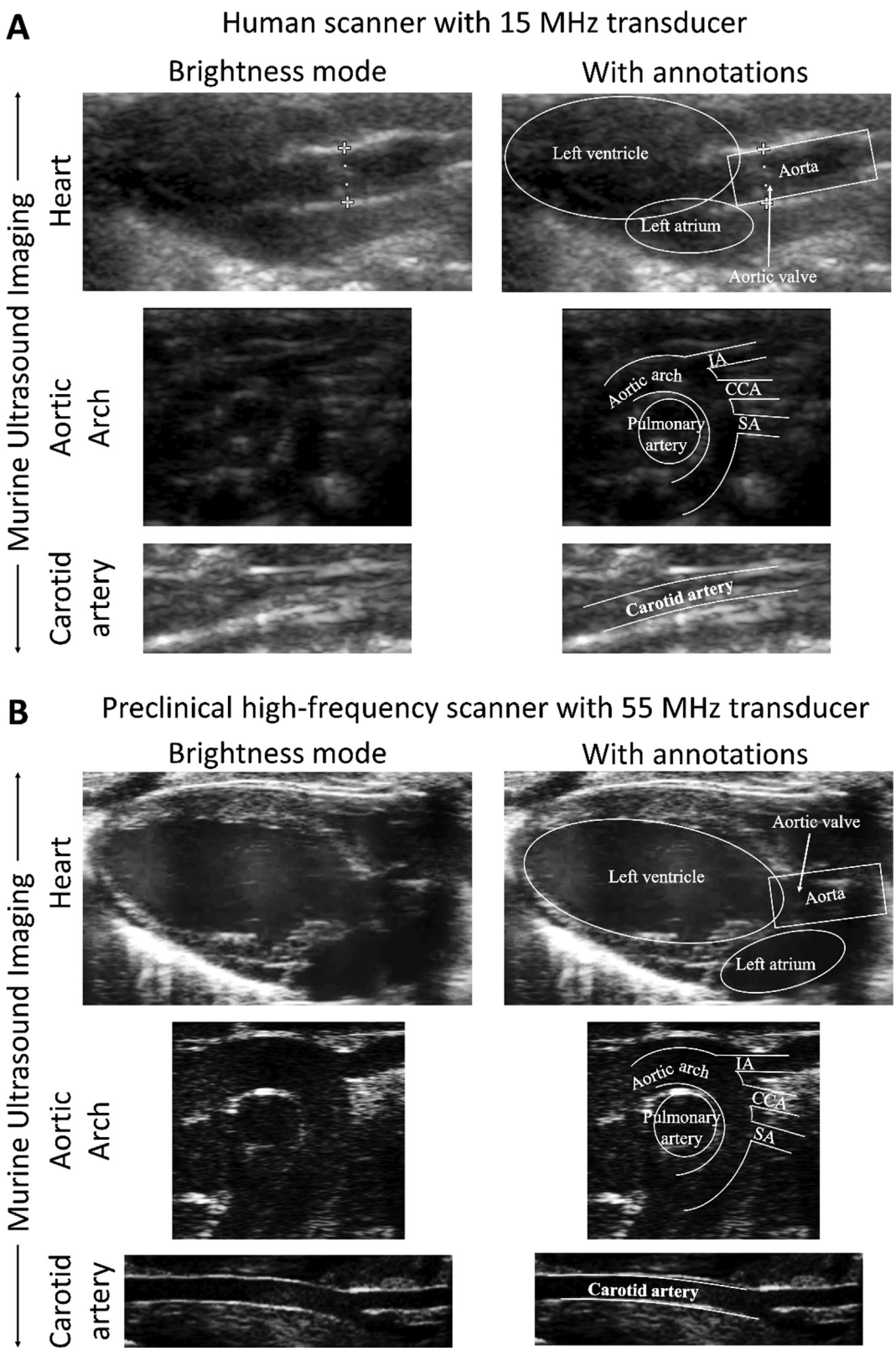

Fig. 1. Ultrasound imaging of a mouse using a clinical scanner and a preclinical high-frequency machine**. A.** Use of a 15 MHz clinical transducer for ultrasound imaging of the heart, aortic arch, and carotid artery resulted in unclear visualization of the anatomy. **B.** Use of a 55 MHz high-frequency transducer for ultrasound imaging of the heart, aortic arch, and carotid artery resulted in clear visualization of the anatomy and definitive vascular structures. **Left**: Brightness mode images. **Right**: Images with annotation of the anatomy. IA, innominate artery; CCA, common carotid artery; SA, subclavian artery.

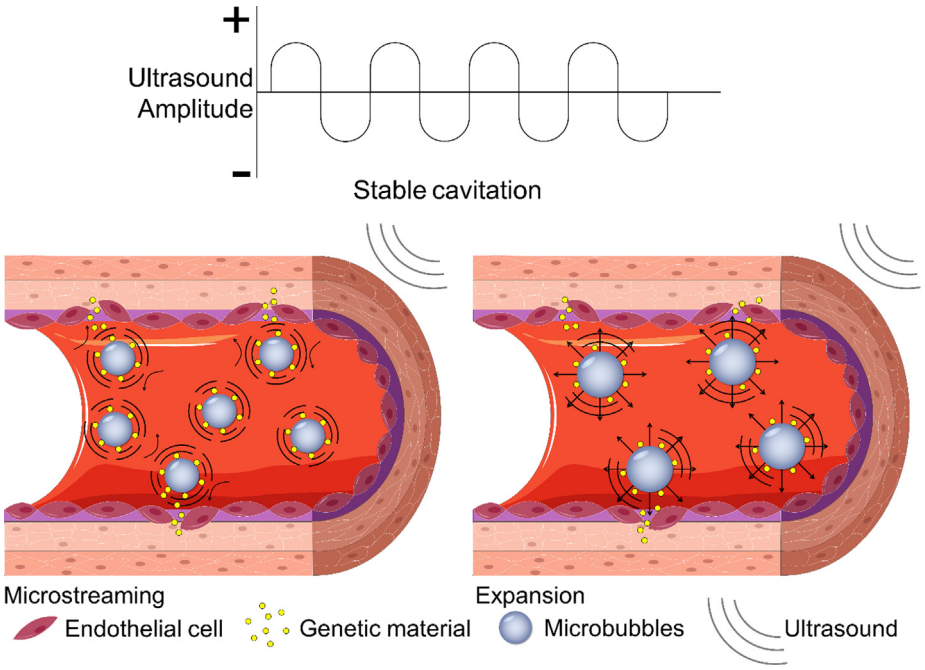

Fig. 2. Schematic diagram showing the effects of low ultrasound amplitudes on ultrasonic particles. Using low-intensity ultrasound makes the gas core of the ultrasonic particles expand and contract, providing a signal for detection by an ultrasound imaging system. The stable oscillation, known as stable cavitation, allows the ultrasonic particles to press against the vessel walls, resulting in an increase in the gaps between endothelial cells. These processes, also known as microstreaming or expansion, result in increased cell permeability and thereby aid in the delivery of drugs and transfection of genetic agents.

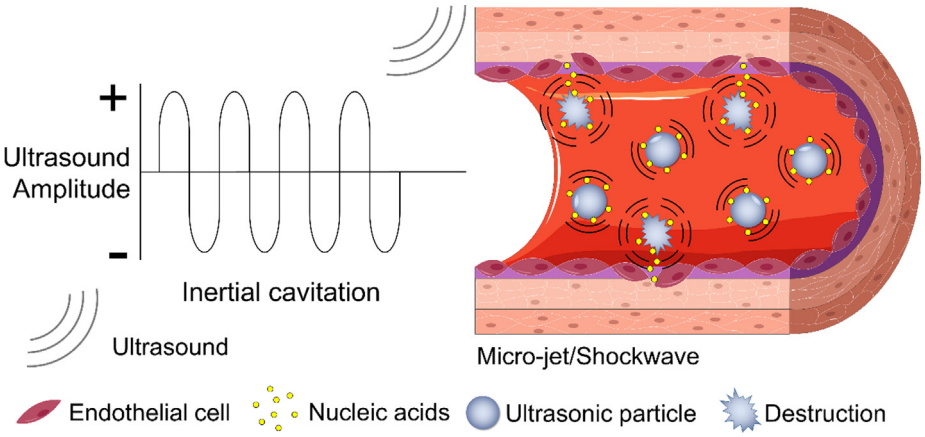

Fig. 3. Schematic diagram showing the effects of high ultrasound amplitudes on ultrasonic particles. Using a high acoustic power setting will cause the oscillation of the ultrasonic particles to become asymmetrical, known as inertial cavitation. When the acoustic pressure is increased to a sufficiently high level, the vigorous oscillations will result in jetting and shockwaves. These phenomena lead to the bursting or destruction of the ultrasonic particles, which also causes mechanical disturbance to the cellular membrane, further increasing permeability and thereby aiding the delivery of drugs and the transfection of genetic agents.

inertial cavitation increase cell permeability, which in turn aid the delivery of drugs and transfection of genetic agents.

5. Delivery of genetic material with microbubbles and ultrasonic nanoparticles

Although the uptake of genetic materials can be enhanced by ultrasound on its own, there are several disadvantages: 1. Off-target effects have been observed when the material is administered systemically. 2. Nucleases in the circulation cause rapid degradation of the genetic materials. 3. There is rapid clearance of the genetic materials from the reticuloendothelial system [53,54]. The use of MBs, liposomes, and other ultrasonic LNPs protects genetic materials from degradation, increases the packaging of materials, and facilitates cellular uptake. MBs usually range between 1 μm and 8 μm in diameter, while most other ultrasonic nanoparticles range between 1 nm and 1 μm. The large size of MBs makes them more suitable for vascular targets because of their difficulty in entering deeper tissues. The development of ultrasonic nanoparticles, including nanoliposomes, nanobubbles (NBs), nanodroplets, and micelles (Fig. 4), allows them to exit vascular confinements and to enter leaky microvasculature and perivascular areas. In terms of their classification, NBs have a gas core, while nanodroplets have a liquid core. Nanodroplets usually encapsulate a low-boiling-point perfluorocarbon or perfluoropentane liquid [55]. Under high acoustic pressure, these nanodroplets are vaporized and become MBs. These ultrasonic particles have been employed for drug and gene delivery over the last two decades.

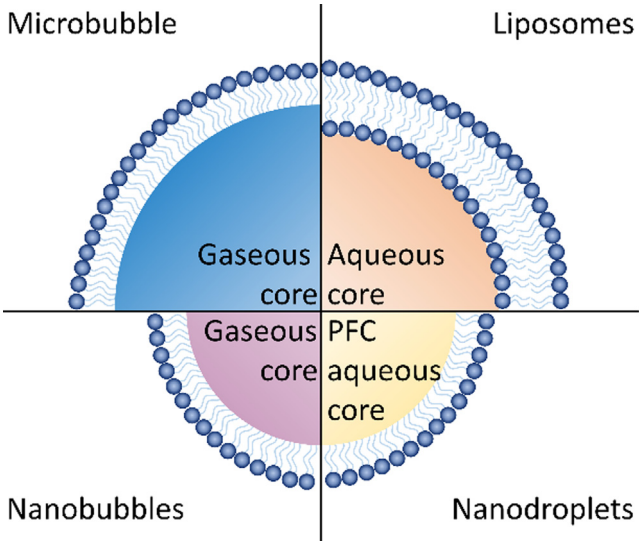

Fig. 4. Schematic diagram showing different types of ultrasonic particles.

6. Ultrasound-targeted gene delivery

The addition of ultrasound-focused techniques activates these ultrasonic particles and achieves targeted gene delivery to the site of exposure, thereby overcoming some of the issues of off-target delivery. This enhancement of drug and gene uptake by the cells is due to the increase in membrane permeability resulting from the combination of ultrasound exposure and ultrasonic nanoparticles [37,56-59]. This method allows for a direct, site-specific transfer of genetic materials into the organ/site of interest and is also termed ultrasound-targeted microbubble destruction, ultrasound-mediated gene delivery, and ultrasound-targeted gene delivery (UTGD). More recently, the employment of these ultrasonic particles, as dual-function contrast agents and therapeutic carriers, has unlocked the development of theranostic strategies (concurrent diagnosis and therapy) [29,60,61]. In addition, conjugation targeting of ligands onto ultrasonic particles allows selective binding of biomarkers to further enhance cell and disease specificity (Fig. 5).

A range of nucleic acids, including plasmid DNA (pDNA), microRNA (miR), mRNA, short hairpin RNA (shRNA), and siRNA, have been used for gene therapy, with most proof-of-concept studies using nucleic acids encoding enhanced green fluorescence protein (eGFP) or luciferase (Table 1 and Table 2). Pioneering research started simply with co-administration of commercial MBs with these nucleic acids followed by ultrasound application. A study noted no difference in UTGD efficacy using two different commercially available MBs, SonoVue and Definity® [62]. A high concentration of unprotected nucleic acids is required because their permeation of the cell membrane is hampered by their negative electrostatic charge and size [63,64]. Unprotected nucleic acids are also recognized as pathogens by the reticuloendothelial system, therefore they face rapid degradation and clearance from the circulation [65].

6.1. Loading nucleic acids onto ultrasonic particles

Further work looked into different formulations of particle shells and cores to package and encapsulate nucleic acids. There are two main strategies to load nucleic acids onto ultrasonic particles: 1) direct conjugation onto the surface or 2) packaging onto cationic polymers nanocomplexes, as a secondary carrier, which is then attached onto the particles. Loading of nucleic acids are performed by exploiting the electrostatic interaction between negatively charged nucleic acids and positively charged lipids, polymers or peptides [66-73]. This coupling improves the stability of the nucleic acid cargo by reducing degradation and removal from circulation, as well as increasing cellular interaction and uptake [58,74].

Using direct coupling of nucleic acids to cationic lipids that form the membrane of the ultrasonic particles, studies have shown increased *in vitro* and *in vivo* UTGD transfection using cationic MBs, as compared to neutral MBs [75,76]. The most commonly used cationic lipids for UTGD include DPPC, DSPC, DOTAP and DOTMA [67,77-79]. While cationic lipids have permanent positive charged head groups, recent studies have also employed ionizable lipids, which exhibit positive charge at low pH and are neutral at physiological pH [80]. Ionizable lipids exhibit better biocompatibility through minimal interactions with blood cells and are the key component of Onpattro, the first FDA approved siRNA drug [80-82]. A

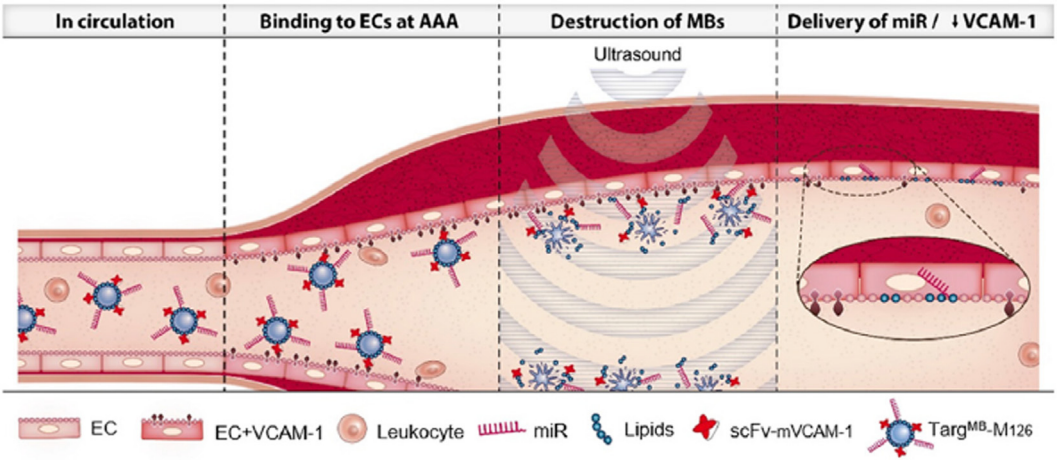

Fig. 5. Schematic diagram showing the mechanism of action for targeted theranostic gene-therapy strategy for treatment of abdominal aortic aneurysm (AAA). Ultrasonic particles, such as microbubbles (MB), were conjugated with single-chain antibodies targeting VCAM-1 (Targ) and miR-126 mimic (M_{126}), resulting in $Targ^{MB}$-M_{126}. In an AAA murine model the vessels were highly inflamed; therefore VCAM-1 is upregulated on endothelial cells. Intravenous injection of $Targ^{MB}$-M_{126} into the circulation allows the particles to locate and bind specifically to inflamed endothelial cells on the vessels. Once $Targ^{MB}$-M_{126} has bound to the inflamed AAA, ultrasound imaging can be performed to visualize the diseased area. Post diagnostic imaging, therapeutic ultrasonic destruction bursts the particles and facilitates M_{126} entering the inflamed cells, thereby providing site-specific therapy [50].

Table 1
In vitro studies.

Cells	Ultrasonic particles (shell and gas core)	Nucleic acids/gene	Ultrasound parameter	Outcome	References
HUH7 cells with stable expression of eGFP & luciferase	DPPC & DSPE-PEG_{2000}-biotin C_4F_{10}	siRNA against luciferase	1 MHz 2 W/cm^2 10% duty 10 s	Higher gene silencing resulting in loss of luciferase signal	Vandenbroucke et al. [103]
3 T3-MDEI, C2C12 & CHO cells	Pluronic block copolymers	pDNA encoding eGFP	1 MHz 1 W/cm^2 20% duty 20 s	Increased transfection efficiency	Chen et al. [105]
Dendritic cells	DPPC, DSPE-PEG-biotin C_4F_{10}	mRNA encoding luciferase or eGFP	1 MHz 2 W/cm^2 50% duty 30 s	Highest luciferase expression observed at 8 h post transfection	De Temmerman et al. [104]
COS-7 cells	DPPC, PEG2000, DOTAP C_3F_8	siRNA against luciferase	2 MHz 2 W/cm^2 50% duty 10 s 2 Hz burst	Downregulation of luciferase expression	Endo-Takahashi et al. [77]
BLM melanoma cells	DPPC, DSPE-PEG-biotin C_4F_{10}	AAV encoding pDNA eGFP	1 MHz 2 W/cm^2 10% duty 10–15 s	Increased internalization of AAV-pDNA into the cytosol but not into the nuclei	Geers et al. [171]
HUVECs	DPPC, DSPEPEG2000-OMe, DSPE-PEG2000-Mal C_3F_8	pDNA luciferase	2 MHz 0.1 W/cm^2 50% duty 10 s 2.0 Hz burst	Significantly higher luciferase expression using AG73 peptide (targeting tumor angiogenic endothelium) particles for UTGD	Negishi et al. [172]

Table 2
In vivo proof-of-concept studies

Disease type	Ultrasonic particles (shell and core)	Nucleic acids/gene	Ultrasound parameter	Outcome	References
Liver imaging, assessing ultrasound kinetics (murine model)	Optison MBs (GE Healthcare)	pDNA luciferase	1 MHz 0–4.3 MPa	Gene enhancement optimum during pressure range of 2–3 MPa	Shen et al. [112]
Liver – long-term gene expression (murine model)	DMAPAP, PEG2000, CHOL C_4F_{10}	pDNA luciferase	1 MHz 930 kPa 20% duty 20 s post-MB injection	Increased luciferase expression of up to 180 days post UTGD	Manta et al. [108]
Kidney tumor experiments (murine model)	DSPC, DSPC-PEG2K, DSPC-PEG2K-Mal C_4F_{10}	pDNA luciferase, eGFP	1 MHz 1 W/cm^2 10% duty	10-fold higher bioluminescence of tumor region	Sirsi et al. [70]
Breast cancer (murine model)	Halobacterium NRC-1 (Halo), PEI air	pDNA eGFP, luciferase	0.6 MPa 50% duty 5 min	Biosynthetic NBs enhanced gene transfection and significantly increased fluorescence intensity	Tayier et al. [85]
Radiation-induced fibrosarcoma-1 – xenograft (murine model)	SonoVue (Bracco) Sonidel MB101 (Sonidel)	pDNA luciferase	1.9 W/cm^2 25% duty 3 and/or 6 min 40 kHz pulse	Expression of luciferase observed throughout the lifetime of the tumor. Tumor size increase was proportional to bioluminescence signal	Li et al. [121]
Intralymphatic imaging (canine model)	DPPC, DSPE-PEG3400 C_4F_{10}	mRNA luciferase	Clinical scanner destruction using mechanical index of 0.61	Unsuccessful delivery of mRNA. Higher power may be needed	Dewitte et al. [173]
Skeletal muscle (murine model)	Optison MBs (GE Healthcare), PEI C_3F_6	pDNA eGFP	1 MHz 3 W/cm^2 20% duty 60 s pulse of 100 Hz	Increased eGFP expression, especially in older (6-month-old) mice	Lu et al. [83]
Skeletal muscle (murine model)	DSPC, DPPE-PEG_{5000}, palmitic acid C_4F_{10}	pDNA luciferase	1 MHz 2 W/cm^2 50% duty	Cationic MBs displayed better transfection than neutral MBs	Panje et al. [67]
Retina (rodent model)	Sonovue (Bracco), PEI	pDNA eGFP	1 W/cm^2 50% duty 1 min	Increased eGFP expression in the retina	Wan et al. [69]

recent review has summarized the uses of these lipids in gene therapy [80]. Others have employed cationic polymers, such as polyethylenimine (PEI) to capture the nucleic acids and form nano-complexes [69,70,83-85]. These complexes are then conjugated on ultrasonic particles for UTGD. The cross-linking of PEI with fluorine-containing alkyl chains to form fluorinated polymers as the outer membrane of nanodroplets [72,73,86], has also been shown to condense and protect nucleic acids from degradation [87].

6.2. Materials and techniques to generate ultrasonic particles

Cationic lipids or polymers have been associated with cytotoxicity, which may be due to their electrostatic interactions with anionic serum plasma proteins [64]. Biocompatible, neutral or helper phospholipids have been incorporated in these particles to reduce toxicity [15,70,80,88-91]. These phospholipids aid in their stability, fusion with the cell membrane, and in promoting the release of nucleic acid in the cytoplasm [92,93]. The incorporation of cholesterol helps stabilize the lipid particle formulation by increasing the packing and reducing the mobility of phospholipid molecules [94].

In addition to the choice of the lipid/polymer layer, many groups have incorporated polyethylene glycol (PEG) into their ultrasonic particles to form a hydrated layer and provide steric stabilization [94]. PEG-particles have been shown to have high biocompatibility and improve *in vivo* dynamics by increasing circulation time [58]. Studies have shown that PEGylated coatings prevent aggregation and reduce phagocytic uptake of the nanoparticles [95]; therefore the half-life of PEGylated nanoparticles can be prolonged from 30 min to 5 h *in vivo* [96].

The internal gaseous or aqueous core of ultrasonic particles also determines their circulating half-life *in vivo*. The use of gaseous or liquid perfluorocarbons is advantageous because of their resistance to biochemical breakdown and their incorporation leads to improved stability. Most micro/nanobubbles are generated using low-solubility perfluorocarbon gases because their low diffusion coefficient and solubility in the blood contribute to longer circulation duration *in vivo*, as compared to particles with an air-filled core [97]. Alternatively, nanodroplets are generated by encapsulating liquid perfluorocarbons and have been demonstrated to be less susceptible to mechanical stress and pressure disparities [97,98]. Echogenicity on ultrasound imaging is also dependent on the size of the ultrasonic particles. Microbubbles of approximately 2 μm provide the optimal acoustic backscatter for imaging [43]. Under ultrasound simulation, these nanodroplets undergo ultrasound-induced droplet vaporization and transition into microbubbles, which result in contrast enhancement and visualization [97]. Nanodroplets, generated with cationic lipids or fluorinated-PEI outer shells [72,73,86], have been shown as ideal theranostic agents because they demonstrate ultrasound contrast properties and can be triggered for efficient gene delivery *in vitro* and *in vivo* [87,99].

A homogenous shell membrane is essential for ultrasonic particles and is commonly achieved via thin-film hydration, reverse-phase or detergent-depletion methods. The thin-film hydration and reverse-phase evaporation methods are used to dehydrate the lipids from their organic solvent [58,100]. The dried film is then rehydrated with physiological buffers containing the substance for encapsulation [58,100]. The generations of ultrasonic particles require mechanical agitation to develop unilamellar and homogenous particles. Techniques such as sonication, extrusion and high-pressure homogenization are employed to further generate sized-controlled ultrasonic particles[27,58,101].

It is important to note that most ultrasonic particles have good gene delivery capabilities on their own and may also achieve low-level genetic transfer without ultrasound stimulation. The addition of ultrasound stimulation will avoid off-target gene delivery by providing a direct, site-specific transfer with increased transfection efficency. Therefore in this review, we focus on UTGD of nucleic acids via ultrasonic particles across a range of diseases.

7. Ultrasound-targeted gene delivery *in vitro*

To achieve an increase in transfection efficiency, the Sanders group first created large biotinylated MBs and small biotinylated cationic liposomes coated with fluorescent-labeled nucleic acids; these were then bridged with avidin to form lipoplexes [102,103]. Using pDNA that encoded luciferase, the group demonstrated successful delivery, transfection, and expression post ultrasound exposure *in vitro* [102]. Using siRNA for gene silencing in cells that expressed luciferase, the authors observed a significant reduction in luciferase expression after the cells were exposed to UTGD [77,103]. UTGD methods were used for the transfection of mRNA encoding luciferase and eGFP into dendritic cells *in vitro* [104]. Using MBs based on pluronics (polymer blocks with customizable lengths), Chen et al. showed increased transfection efficiency of pDNA into fibroblasts, myoblasts, and endothelial cells when combined with ultrasound *in vitro* [105]. Other *in vitro* work by Yang et al. silenced P-glycoprotein using shRNA coated on doxorubicin-encapsulated NBs via UTGD and demonstrated increased cytotoxicity of human breast cancer cells with adriamycin resistance [106]. Overall, *in vitro* UTGD has been well established and is frequently used as a proof of concept for the properties of ultrasonic particles and their transfection efficacy. However, the transition into *in vivo* applications requires many optimization steps, specific to the anatomical location of the tissue/organ and its composition.

8. Ultrasound-targeted gene delivery *in vivo*

8.1. Safety and specificity

The safety of UTGD has been evaluated in several studies. *In vivo* models have also been employed to determine whether the destruction and cavitation of ultrasonic agents lead to tissue damage. Many of the studies chose to use pDNA encoding luciferase to determine gene expression and to measure changes in liver enzymes as an indicator of hepatic damage. While some studies have raised concerns in relation to elevated enzymatic measurements [107], most studies have indicated no or minimal tissue damage [108-111].

Noble et al. documented increased luciferase expression in the liver in an *in vivo* canine study [107]. In this proof-of-concept study, the authors found that luciferase expression in some tissue sections produced up to an 1800-fold enhancement compared with the sham-treated animals [107]. The authors noted minor liver damage in areas that were exposed to therapeutic ultrasound via elevated liver enzyme levels and on histological studies. However, the central lobe, which was exposed to diagnostic ultrasound, was not affected [107]. However of the nine dogs used in this study, each varied in relation to the amount of MBs administered, the route or time of injection, the choice of transducer or its peak negative pressure, and the total treatment time. Therefore, it is important to note that for each specific therapy, there was only one sample. There is clearly a need to perform more experiments to determine the safety of their UTGD approach *in vivo* before we can draw a conclusion.

In a murine study using Optison MBs, Shen et al. noted that the optimum peak negative pressure ranged between 2 and 3 MPa, and resulted in an 85-fold increase in luciferase expression [112]. However, the authors did not look at possible liver damage in this study. Manta et al. observed prolonged luciferase expression in the liver for 180 days, but noted that UTGD caused damage to the liver cells in the first 2 days [108]. However, the liver enzymatic levels returned to normal by day 7 [108]. These findings highlight the potential of using UTGD for long-term therapy. Nevertheless, increased amplitudes have been associated with higher degrees of tissue damage [113], therefore there is a need to optimize the ultrasound pressure amplitudes required. Many groups have also investigated the use of optical UTGD and have reported

Table 3
Neurodegenerative and muscular diseases

Disease type	Ultrasonic particles (shell and core)	Nucleic acids/gene	Ultrasound parameter	Outcome	References
Huntington's disease (murine model)	SonoVue MBs (Bracco)	pDNA GDNF	1 MHz 1% duty 30 s	Significant neuroprotective effect and improved motor ability	Lin et al. [127]
Huntington's disease (murine model)	DSPC, Bio-DSPE-PEG2000 C_3F_8	pDNAs GDNF & Nurr1	1 MHz 2 W/cm^2 20% duty	Improved behavior scores and immunohistochemical staining showed increased levels of tyrosine hydroxylase and dopamine transporter	Yue et al. [130]
Parkinson's disease (rodent model)	DPPC, DSPE-PEG2000, DPTAP C_3F_8	pDNA GDNF	1 MHz 0.7 MPa	Neuroprotective effect in mice with restored behavior function	Fan et al. [129]
Duchenne muscular dystrophy (murine model)	DPPC, DSPE-PEG2000-OMe C_3F_8	Antisense PMO	1 MHz 2 W/cm^2 50% duty 60 s	Increased PMO-mediated exon-skipping efficiency and enhanced dystrophin expression	Negishi et al. [123]
Duchenne muscular dystrophy (murine model)	DSPE, PEG2000, DPPC C_3F_8	Antisense PMO	1 MHz 2 W/cm^2 50% duty 60 s	Recovered dystrophin expression in the targeted skeletal muscle	Negishi et al. [124]
Spinal cord injury (rodent model)	DPTAP, DPPC, DSPE-PEG-COOH C_3F_6	pDNA BDNF	1.5 W/cm^2 5 min	Significant neuroprotective effect on the injured spinal cord with decreased level of apoptosis	Song et al [126]

no histological tissue damage to the retina or the sub–conjunctival tissues, or any other adverse effects [69,114-116].

8.2. Liver diseases

Ultrasound imaging is already commonly used for diagnosis of liver disease, including fatty liver and fibrosis. As a result, UTGD for liver diseases is widely studied. In a rodent model of liver ischemia/reperfusion (I/R) injury where Yan et al. co-injected siRNA against heat shock protein 72 with MBs, ultrasonic irradiation resulted in a smaller degree of liver injury [117]. Using *in vivo* models of liver fibrosis, UTGD of hepatocyte growth factor has been shown to produce an anti-fibrosis effect, preserve the lobule structures, and result in smaller amounts of fibrous septum as compared to controls [118,119]. Furthermore, Jiang et al. showed that this therapy directly resulted in a significant reduction in liver enzyme levels [118]. Zhang et al. demonstrated in the same rodent model that UTGD of hepatocyte growth factor and transforming growth factor β improved liver function, reduced the severity of hepatic fibrosis, and promoted the regeneration of liver cells [120]. These studies indicated that UTGD provided liver protection without tissue damage. Together with the frequent usage of ultrasound for liver imaging, these preclinical studies provide substantial proof of concept data for future clinical translation of UTGD in the therapy of hepatic conditions.

8.3. Muscular diseases

The murine hindlimb skeletal muscle model is well established and widely used for the investigation of gene transduction. Using this *in vivo* model, Panje et al. investigated the transfection efficiency of firefly luciferase pDNA using either cationic or neutral MBs [67], indicating that ultrasound exposure and surrounding MBs were sufficient to facilitate transfection. A separate experiment showed that UTGD resulted in prolonged gene expression *in vivo* in the hindlimb for up to 84 days after a single intramuscular injection of pDNA and MBs [121], demonstrating the potential for sustained therapeutic benefits. Since the simple co-administration of MBs and nucleic acids has been associated with cellular damage, Lu et al. demonstrated that there was less tissue damage with incorporation of the cationic polymer PEI [83].

Using UTGD on the tibialis anterior (TA) muscle, after intramuscular injection of acoustic liposomes and 10 ug of pDNA encoding luciferase Wantanabe et al. observed much higher *in vivo* bioluminescence signal post therapy [122]. Using a gamma counter to measure the uptake of the iodine-124 isotope radiotracer, biodistribution studies indicated localization of gene expression in the TA muscle. Regions received pDNA encoding sodium/iodine symporter genes, acoustic liposomes, and ultrasound exposure [122]. The successful transfection of this pDNA and its expression were further confirmed 4 days post therapy using positron emission tomography imaging to image the uptake of the sodium-124 isotope in the TA muscle [122].

Duchenne muscular dystrophy, a fatal condition and the most common pediatric neuromuscular disease, has been of major interest in relation to genetic therapy approaches (Table 3). Using bubble liposomes coupled with phosphorodiamidate morpholino oligomer (PMO), Negishi et al. demonstrated successful gene therapy *in vivo* in a murine model of Duchenne muscular dystrophy [123,124]. After intramuscular injection into TA muscle tissue and targeted ultrasound, the group observed an increase in the number of dystrophin-positive fibers via immunofluorescence microscopy [123]. However, in this article controls for the bubble liposomes + PMO without ultrasound as well as the PMO + ultrasound were not presented. Therefore it is difficult to determine the efficacy of the combination without relevant comparison to the needed controls. Direct intramuscular injections and UTGD have shown successful gene transfection to the muscle of interest. Although further research must be conducted to ensure effectiveness and safety, the simplicity of the UTGD on skeletal muscle makes this technology ideal for the treatment of Duchenne muscular dystrophy and may lead to an early prospect for clinical translation.

8.4. Fetal diseases

A common X-linked genetic disorder of the urea cycle in infants is related to ornithine transcarbamylase (OTC) deficiency. Since OTC is a single-gene defect, researchers have been investigating whether the repair and/or replacement of this defective gene might offer a therapeutic alternative to liver transplantation [125]. Using OTC-deficient female mice, Oishi et al. generated heterozygous pregnant mice. On day 16 of gestation, an incision

was made to the abdominal to expose the uterus, where the authors directly injected the liver of the fetus with 5 μg of pDNA encoding OTC and 1.25 μL of Sonazoid MBs [125]. Following the injection, UTGD was performed directly on the fetal liver through the uterus wall at 1 W/cm^2 at 50% duty for 30 s. The authors observed decreases in the blood ammonia level and the urinary orotic acid:creatine ratio in the treatment group of hemizygous males at 3 days after birth [125]. It was also noted that the *ex vivo* liver specimens that underwent gene therapy using sonoporation measured an increase in OTC activity at pH 9.5, as compared to pH 7.7, although the mechanism or reasoning for this association is uncertain [125]. One possible explanation suggested was that UTGD might induce structural changes which resulted in more efficient functionalisation at higher pH levels [125]. Delivering therapeutics to the developing fetus requires consideration of both mother and fetus, as well as to account for any immunological responses that may occur. While more research into their safety is required, these challenges may be overcome by UTGD to facilitate targeted treatment directly to the fetus without off-target effects on the mother.

8.5. Spinal cord and neurodegenerative diseases

Another emerging area for gene therapy is the field of spinal cord injury and neurodegenerative diseases (Table 3). Song et al. generated NBs that were targeted to the neuron-specific molecular marker microtubule-associated protein 2 for the delivery of a plasmid-encoding brain-derived neurotrophic factor (BDNF) [126]. Using an acute spinal cord injury rodent model where the contusion injury was induced on the 10th thoracic segment, the rats underwent 5 min of UTGD every 12 h for 3 days. The authors demonstrated increased BDNF gene and protein expression post UTGD treatment *in vitro* and *in vivo* [126]. Furthermore, the rats that underwent this treatment exhibited normal morphology, increased regenerative axons, and increased values on the Basso, Beattie, and Bresnahan locomotor rating scale for behavioral consequences, as well as decreased neuronal necrosis and smaller lesion cavity areas [126]. Overall, this study demonstrated UTGD successfully provided neuroprotection on the injured spinal cord.

The brain is a complex target for most therapies because of the difficulty in penetrating the blood–brain barrier. To rectify this, groups have investigated the use of MB-facilitated focused ultrasound in an attempt to generate temporary openings [127,128]. By employing pDNA encoding glial cell line–derived neurotrophic factor (GDNF) coupled onto liposomes, Lin et al. demonstrated MBs opening the blood–brain barrier and achieved gene therapy in the brain in a mouse model of Huntington's disease *in vivo* [127]. They observed significant improvement in motor ability in treated mice, as well as a neuroprotective effect that retarded disease progression, evidenced by neuroanatomical and motor function observations [127]. In the field of Parkinson's disease, patients have decreased GDNF and orphan nuclear receptor Nurr1 [53,129-131]. UTGD delivery of pDNA encoding GDNF in a rodent model of Parkinson's disease resulted in neuroprotection and restored behavior functions [129]. With the same animal model, Yue et al. created two pDNAs encoding either GDNF or Nurr1 that were then packed separately or together into biotinylated liposomes and conjugated onto MBs for MRI-guided ultrasound therapy [130]. Post disease induction, the rats were subjected to therapy every 3 days for 3 weeks [130]. The animals treated with both plasmids produced improved behavior scores and their immunohistochemical staining showed increases in levels of tyrosine hydroxylase and dopamine transporter [130]. The above study demonstrated that ultrasonic particles aid the delivery of gene therapy in the brain and successful provide neuroprotection in the animals. The ability of UTGD to temporarily open the blood–brain barrier has the potential to be a ground-breaking development, with ramifications for many neuronal degenerative diseases.

8.6. Ophthalmic and retinal diseases

Genetic therapy is ideal for a variety of ophthalmic and retinal diseases because of its accessibility and favorable immunological properties in relation to being immune privileged. In a proof-of-concept study, Sonoda et al. performed UTGD by simultaneously using commercially available MBs (Optison) and pDNA encoding eGFP *in vitro* in cultured rabbit corneal epithelial cells and *in vivo* by co-administering them to New Zealand albino rabbits [132]. The authors observed more eGFP-positive cells in the targeted regions of the corneal stroma of animals receiving UTGD than in those that received plasmid injections alone, received Optison alone, or were just subjected to ultrasound bursts [132].

Wan et al. generated PEI-conjugated eGFP pDNA and demonstrated increased eGFP expression in cultured human retinal pigment epithelial cells *in vitro* when delivered using commercially available MBs (Sonovue) and UTGD [69]. The authors also observed a strong positive eGFP signal after co-administering MBs with PEI-conjugated eGFP pDNA and UTGD in Sprague-Dawley rat retinas *in vivo* [69]. In another study, Sonoda et al. investigated transfer of the eGFP plasmid via intravitreal ultrasound irradiation to the retina *in vivo* using pDNA-coated PEG-liposomes containing perfluoropropane gas [84]. The authors observed a significant increase in the number of eGFP-positive cells in the retinas of the rabbits, exclusive to the area exposed to ultrasound [84]. The probe used in this study was approximately the size of a 19-gauge needle [84], indicating that this intravitreal UTGD may be more selective than most other methods. The same group also demonstrated an increase in eGFP signal in the conjunctiva of rats *in vivo* after UTGD [114].

Importantly, these groups found no adverse effects and no histological tissue damage on the retina or the sub–conjunctival tissues [69,114]. However, while UTGD may be a safe procedure for ophthalmic and retinal diseases, most of these studies have only used nucleic acids encoding for eGFP or luciferase. Therefore it is still unknown whether this approach may provide a clinical benefit to vision.

8.7. Malignant diseases

Genetic therapy for malignant diseases has been heavily explored (Table 4). Using Balb/c-nu Slc nude mice, Sakakima et al. treated subcutaneously implanted hepatocellular carcinoma solid tumors with pDNAs encoding eGFP, interferon-β (IFN-β), and β-galactosidase (LacZ) by ultrasound MB-targeted delivery [133]. In *in vitro* assays, the authors showed only 24% transfection efficacy when using sonoporation of commercially available MBs and 10 μg of eGFP pDNA on SK-Hep1, human hepatic adenocarcinoma cells [133]. The group further observed that 60% of the nodules (12/20 nodules) had a reduction in tumor size *in vivo* 4 weeks post UTGD using MBs and 50 μg of IFN-β pDNAs [133]. In end point histology, terminal deoxynucleotidyl transferase dUTP nick end labeling (TUNEL) staining was used to demonstrate apoptotic induction in subcutaneous tumors that underwent sonoporation, further indicating that the anti-tumor effect of the IFN-β gene may have inhibited tumor growth [133].

Similarly, UTGD was employed to deliver pDNA encoding interleukin (IL)-27 *in vivo* and showed significant tumor size reduction (50–75%) across three different models of immune-competent prostate adenocarcinoma [134]. Suzuki et al. used 1,2-distearoyl-*sn*-glycero-3-phosphorylethanolamine (DSPE) and 1,2-distearoyl-*sn*-glycero-3-phosphoethanolamine-N-[polyethylene glycol-2000] (DSPE-PEG2000) to form the lipid shell of liposomes via sonication

Table 4
Malignant diseases

Disease type	Ultrasonic particles (shell and core)	Nucleic acids/gene	Ultrasound parameter	Outcome	References
Breast cancer – xenograft (murine model)	DPPC, DSPE-PEG2000-Biotin, DSPE-PEG2000, DC-CHOL C_3F_8	pDNA CD105 (endoglin)	1 MHz 1 W/cm^2 50% duty 30 s	Significantly smaller tumor size with decreased level of angiogenesis	Zhou et al. [76]
Breast cancer – xenograft (murine model)	PEGylated species DPPC and DSPC C_4F_{10}	siRNA cell-penetrating peptides	1 MHz 1 W/cm^2 10 s sonication + 10 s pause for a total of 60 s	c-Myc silencing and inhibition of tumor growth	Xie et al. [142]
Adrianmycin-resistant breast cancer – xenograft (murine model)	mPEG-PLGA-PLL, PEAL water	siRNA against ABCG2	1 MHz pulse of 100 Hz	UTGD with siRNA that silenced breast cancer resistance protein (ABCG2), together with adriamycin, resulting in stronger inhibition of tumor growth	Bai et al. [145]
Hepatocellular carcinoma – xenograft (murine model)	BR-14 MBs (Bracco)	pDNA IFN-β	1 MHz 2 W/cm^2 50% duty	UTGD of IFN-β resulted in decreased tumor size	Sakakima et al. [133]
Hepatocellular carcinoma – xenograft (murine model)	mPEG-NH_2, C_9F_{17}-NH_2 Perfluoro-*n*-pentane	miRNA miR122	1 MHz 1.2 W/cm^2 20% duty 1 min	Suppression of tumor growth and proliferation	Guo et al. [141]
Hepatocellular carcinoma – xenograft (murine model)	DPPC, DSPE, DPPA C_3F_6	pDNA HSV-TK (suicide gene)	1 MHz 2 W/cm^2 5 min 10 s interval time	Significantly higher apoptosis of cancer cells, improved anti-tumor effects and survival	Zhou et al. [137]
Hepatocellular carcinoma – xenograft (murine model)	SonoVue MBs (Bracco)	pDNA HSV-TK (suicide gene)	1 MHz 2 W/cm^2 5 min	UTGD together with ganciclovir treatment increased apoptosis index, reduced tumor growth and improved survival	Nie et al. [138]
Hepatocellular carcinoma – xenograft (murine model)	Egg PC, DPPG, DPPE, CHOL 0^2	pDNA HSV-TK or Timp3 genes	1.3 MHz 5 min 1 s interval time	Individual gene therapy with HSV-TK or Timp3 genes resulted in 45% suppression of tumor growth and increased survival. Further 30% improvement was achieved with co-delivery	Yu et al. [174]
Hepatocellular carcinoma – xenograft (murine model)	DSPC, DPPA, DSPE-PEG2000, PEI SF_6	shRNA against survivin	1 MHz 1.1 W/cm^2 50% duty 1 min	Reduced tumor volume with decreased survivin expression	Li et al. [175]
Doxorubicin-resistant hepatocellular carcinoma – xenograft (murine model)	BR38 MBs (Bracco) with PLGA NP	miRNA miR122, anti-miR21	Clinical transducer	Synergistic treatment with doxorubicin resulted in ~ 27% apoptosis in resistant tumors, 6-fold greater than using doxorubicin alone	Mullick Chowdhury et al. [146]
Metastatic melanoma (rodent model)	DSTAP, DSPC, NH2-PEG2000-DSPE or man-PEG2000 C_3F_6	pDNA pUb-M murine melanoma GP-100 & TRP-2	1.045 MHz 1 W/cm^2 50% duty 10 Hz burst rate 2 min	Enhanced secretion of Th1 cytokines (IFN-γ and TNF-R) was observed in splenic cells. Suppression of pulmonary metastatic tumors post induction was achieved	Un et al. [149]
Colon or pancreatic cancer – xenograft (rodent model)	PLGA Core not specified	pDNA p16 (tumor suppressor gene)	Color Doppler mode with a mechanical index of 1.5	Reduced doubling time of tumors	Hauff et al. [136]
Human cervical cancer – xenograft (murine model)	DPPE, DSPE, DPPA C_3F_8	siRNA against X-linked inhibitor of apoptosis protein	1 MHz 1 MPa 50% duty	Increased gene-silencing effect with decreased cancer cell density and increased pro-apoptotic components	Wang et al. [71]
Human cervical cancer – xenograft (murine model)	SonoVue MBs (Bracco) PEI	shRNA against human survivin gene	3 MHz 2 W/cm^2 20% duty 2 min	Successful inhibition of survivin after UTGD via shRNA resulting in cancer cell apoptosis	Chen et al. [111]
Prostate cancer – xenograft (murine model)	DPPC, DSPE_PEG2000-COOH, DC-CHOL C_3F_6	siRNA against forkhead box M1	1 MHz 2 W/cm^2 50% duty	Inhibited tumor growth and prolonged survival rate	Wu et al. [147]
Prostate cancer – xenograft (murine model)	SonoVue MBs (Bracco)	pDNA IL-27	1 MHz 1 W/cm^2 50% duty 45 V 2 HZ on specified intervals	Reduction in cell viability, with 50% to 75% reduction in tumor growth	Zolochevska et al. [134]
Drug-resistant testicular cancer (rodent model)	Not specified	siRNA against MDR1 gene	300 kHz 2 W/cm^2 10 min	UTGD of siRNA against MDR1 gene, together with daunorubicin, significantly reduced testicular tumor volumes	He et al. [144]

and constructed ultrasonic liposomes via supercharging with perfluoropropane gas. UTGD using these ultrasonic particles to deliver pDNA encoding IL-12 resulted in effective tumor suppression, while in 80% of the mice it achieved complete regression [135]. No anti-tumor effects were noted for the control groups treated with the DNA alone, with ultrasonic particles, with ultrasound, or with a commercially available transfection agent, lipofectamine 2000 [135]. In addition, UTGD with pDNA encoding the tumor suppressor gene p16 or the herpes simplex virus thymidine kinase suicide gene has also significantly slowed tumor growth and increased survival rates *in vivo* [136-139].

In a recent study, Dong et al. fabricated sponge-loaded magnetic nanodroplets for the delivery of microRNAs (miRNAs). These targeted the miR-515 family, resulting in an *in vivo* therapeutic effect of tumor shrinkage post simulation with focused ultrasound [140]. These nanodroplets were produced by dispersing fluorinated iron oxide nanoparticles (SPIO-NPs) in a perfluorocarbon- coated cationic lipid shell and coating them with miRNA sponges. For therapy, the placement of a magnet on top of the tumor enabled magnetism-assisted targeting of the non-biomarker-targeted nanodroplets. After more than 6 h of magnetism-assisted targeting, focused ultrasound was performed on xenograft tumors. In addition to the reduction in tumor size, immunohistochemistry also demonstrated an increase the expression of anti-oncogenes in the cancer cells [140]. Using miR122 and nanodroplets, Guo et al. also demonstrated that UTGD successfully suppressed tumor growth and inhibited proliferation *in vivo* [141].

In addition to lipid-based ultrasound particles, some groups have incorporated the cationic polymer PEI into their formulation for nucleic acid delivery [70,111]. Sirsi et al. coupled luciferase pDNA to PEI-coated MBs and demonstrated *in vivo* successful transfection into tumors that were implanted in the kidneys of mice [70]. Using PEGylated-PEI-SH, the thiol group was covalently conjugated onto the MB shell using the maleimide group on DSPC-PEG2K-Mal lipid. Ultrasound was performed directly on the kidney region [70]. Post transfection, *in vivo* bioluminescence imaging showed an over 10-fold higher signal from the tumor region compared to untreated tissue [70].

A study by Xie et al. conjugated siRNA against the human c-Myc gene to cell-permeable peptides. These were then entrapped in NBs and addition of ephrin mimetic peptide enabled targeting to EphA2-positive human breast adenocarcinoma cells [142]. Post UTGD, increased transfection was observed within the tumor region, resulting in further strong anti-tumor effects *in vivo* [142]. CD105, endoglin transmembrane glycoprotein, is highly expressed within endothelial cells in breast cancer and hence were the target for UTGD. This therapy resulted in a 24.7-fold increase in transfection efficacy *in vitro* and successful delivery of pDNA encoding human endostatin, which inhibited tumor growth *in vivo* [76]. UTGD and siRNA have also been used to silence the isocitrate dehydrogenase 1 gene and the multidrug-resistant protein 1 gene *in vivo*, resulting in significant reductions in the sizes of glioma and testicular tumors respectively [143,144]. Since multidrug resistance presents an issue in cancer therapy, UTGD's ability to silence or alter these resistant cells may also aid their effectiveness *in vivo* [144-146].

Wang et al. generated siRNA micelles by coupling the siRNA with a cationic diblock copolymer to increase encapsulation efficiency and to protect them from exposure to ribonuclease [71]. Prior to UTGD, these cationic micelles were directly incorporated onto MBs by incubation. The authors used siRNA against the X-linked inhibitor of apoptosis protein to investigate the anti-cancer effect on tumor-bearing mice via direct intratumoral injection on days 1, 4, 7, and 10 [71]. Mice treated with UTGD of siRNA-conjugated MBs showed a decrease in tumor size and increased survival [71]. The authors reported that 16.7% of mice in this treatment group died from loss of weight, a phenomenon that was not reported from their other control groups [71]. They stated that the reason for these deaths was unclear, so more rigorous investigation might be needed to determine safety.

An increase in survival was also observed in an *in vivo* study using gene silencing of forkhead box M1 transcription factor [147]. The group loaded siRNA onto cationic NBs and conjugated them with A10-3.2 aptamers which targeted the prostate-specific membrane antigen expressed on human prostate cancer cells [147]. A substantially slower tumor growth rate was noted in tumor-bearing mice which underwent these UTGD treatments every 3 days for a total of 7 times [147]. Another interesting approach to UTGD is the utilization of bacteria-produced, gas-filled, proteinaceous nano-compartments as biosynthetic NBs. Incubation of these biosynthetic NBs with cationic PEI allowed for electrostatic loading of eGFP and/or luciferase gene reporter pDNA [85]. In a proof-of-concept *in vivo* subcutaneous xenograft murine model, Tayier et al. observed increased bioluminescence signals in the tumor areas post UTGD treatment [85].

Gene therapy has also been frequently studied in relation to treating chronic inflammation. Un et al. generated mannose-binding polyethylene glycol-2000 bubbles (Man-PEG2000 lipoplexes) for the delivery of luciferase- or ovalbumin-expressing pDNA [148]. Since mannose receptors are abundantly expressed on antigen-presenting cells, these Man-PEG2000 lipoplexes selectively targeted hepatic non-parenchymal cells and splenic dendritic cells. Using lymphoma cells expressing ovalbumin (E.G7-OVA), the authors demonstrated anti-tumor activity by increasing cytotoxic T lymphocytes via ovalbumin-coated Man-PEG2000 lipoplexes and ultrasound exposure [148]. The group then performed 3 doses of immunization at weeks 0, 2, and 4 prior to E.G7-OVA cell tumor induction *in vivo* in week 6, and demonstrated an increase in survival rate and a decrease in tumor size [148]. Using a similar immunization timeline, as well as the same Man-PEG2000 lipoplexes and ultrasound settings, the group investigated an *in vivo* metastatic murine model using a pDNA co-expressing murine melanoma glycoprotein-100 and tyrosinase-related protein-2 [149]. Suppression of pulmonary metastatic tumor post-induction with B16Bl6 melanoma cells was observed [149]. It is worth noting that a high volume of 400 μL of lipoplexes was injected into each mouse for the *in vivo* gene transfection study.

Clinically, the vast number of mechanisms by which cancers may arise complicate their treatment. The above preclinical studies demonstrate the clear potential for UTGD treatment across a multitude of solid cancers and metastases. Notably, the studies showcase the flexibility of the ultrasonic particles and the choice of gene therapy available, as well as the use of UTGD and their potential to be employed for personalized medicine to develop treatment strategies tailored to individual cancer cases.

8.8. Inflammatory diseases

During inflammation, Kupffer cells and hepatic endothelial cells also express the mannose receptor, so these Man-PEG2000 lipoplexes can be repurposed for anti-inflammatory therapy. Crohn's disease, a chronic inflammatory disease of the gastrointestinal tract, may be suited for gene therapy. In another proof-of-concept study using TNFΔARE mice, which are an animal model of inflammatory bowel disease–like disorders, Tlaxca et al. demonstrated successful gene transfection using MAdCAM-1 or VCAM-1 targeted MBs [150]. These MBs were loaded with luciferase gene pDNA resulting in an increased bioluminescence signal in the gut post UTGD [150]. Inflammation is the root cause of many diseases, including allergy, asthma, atherosclerosis-related cardiovascular diseases and multiple sclerosis [46,151,152], therefore, further

investigation of UTGD for inflammation and their targets may offer therapy to a board range of downstream medical issues.

8.9. Cardiovascular diseases

Cardiovascular diseases (CVDs) such as ischemic heart disease, heart failure, stroke, and vascular diseases are the largest cause of death worldwide [153]. Therefore many groups have investigated the use of UTGD for long-term therapy (Table 5). For patients who are suffering end-stage heart failure, often their only chance of survival is a heart transplant. However, acute cardiac rejection results in 20% mortality in the first year post heart transplant [154]. Using antagomir-155 delivered via MBs and UTGD, Yi et al. observed an attenuation of acute cardiac rejection in a mouse *in vivo* setting [78]. In this study, the MBs were synthesized via the sonication method using distearoylphosphatidylcholine (DSPC), 1,2-dioleoyl-3-trimethylammonium propane (DOTAP), and DSPE-PEG2000 with perfluoropropane gas. UTGD resulted in targeted delivery of antagomir-155 into the murine allograft hearts, downregulated miRNA-155, and the downregulation of several cytokines and inflammatory markers [78]. Similar findings were reported in a recent rodent study using UTGD of galectin-7 siRNA on days 1, 3, 5, and 7 post cardiac transplantation [154]. Wang et al. observed reduced cardiomyocyte apoptosis, attenuated inflammatory infiltration and myocyte damage, and minimal immune rejection in the targeted therapy group [154]. Compared to currently used clinical strategies using broad-scale immunosuppressant therapeutics and their associated side effects, UTGD shows great promise in reducing organ rejection with reduced risk.

In addition to finding ways to prevent rejection, there is a need to discover new therapeutic and prophylactic approaches to CVDs. Zhang et al. demonstrated that UTGD of shRNA, which silences the oxygen-dependent prolyl hydroxylase-2, resulted in a better outcome after I/R in a rodent model [155]. The MBs were produced with dipalmitoylphosphatidylcholine (DPPC), DC-cholesterol (DC-CHOL), and DSPE-PEG2000 by sonication with octafluoropropane gas, followed by coupling of 18 μg of pDNA per 5×10^8 MBs. Using a rodent myocardial I/R model where the left anterior descending coronary artery was ligated for 10 min, the MBs were administered to rats on day 0 and day 4 for UTGD. On histology, the short-term outcome (48 h post treatment) showed fewer apoptotic cells in the infarct area, while the long-term outcome (4 weeks post treatment) showed decreased infarct size [155].

Wang et al. showed increased expression of vascular endothelial growth factor (VEGF) protein and angiogenesis in the myocardium of rats that underwent myocardial I/R injury, after treatment with UTGD of VEGF-coupled MBs [156]. However, in this study the authors only looked at the histological endpoint and it is unclear if there was improvement to the function of the heart. The improvement of cardiac function after myocardial I/R injury has been reported by several groups post gene therapy via UTGD *in vivo*. Fujii et al. demonstrated that a single dose of gene therapy with pDNA coding for either VEGF or stem cell factor (SCF), given 7 days after full ligation of the left coronary artery, both resulted in increased ejection fraction as measured via echocardiography [157]. However, 2 years later the group followed up with a myocardial I/R model that required 6 sessions of gene therapy using pDNA encoding for SCF and stromal cell–derived factor-1α to achieve increased vascular density, increased ejection fraction, and decreased infarct size [158]. The difference between the number of sessions needed for the 2 studies was not discussed; however, it may be worth noting that the former study was in mice, whereas the latter study was in rats. It is also unclear why Troponin I, a clinical marker of MI, was not increased in the blood of the rodents post I/R injury in the latter study.

In another myocardial I/R rodent model, UTGD of a protein kinase B (AKT) plasmid was investigated by Sun et al. using both commercially available Definity MBs and octafluoropropane

Table 5
Ischemic and cardiovascular diseases

Disease type	Ultrasonic particles (shell and core)	Nucleic acids/gene	Ultrasound parameter	Outcome	References
Hindlimb ischemia (rodent model)	PEG-40 stearate, DSPC, DSTAP C_4F_{10}	miRNA miR126	1.3 MHz 0.9 W/cm^2 5 s interval	Significant improvement in microvascular perfusion	Cao et al. [163]
Iliac artery intimal proliferation (rabbit model)	BSA, sucrose O2 & C_3F_8	Antisense PNA	1 MHz 1.5 W/cm^2 6 min	Reduced smooth muscle cell proliferation	He et al. [162]
Liver I/R (rodent model)	Sonovue MBs (Bracco)	siRNA HSP72	2.5 MHz MI 1.0	Reduced liver injury and necrosis in treatment group, with lower plasma levels of ALT, HSP72, and TNF-α	Yan et al. [117]
Allograft hearts (murine model)	DSPC, DOTAP, DSPE-PEG200 C_3F_8	miRNA antagomir155	2 MHz 2 W/cm^{-2} 50% duty	Attenuation of acute cardiac rejection and increased survival time	Yi et al. [78]
Allograft hearts (rodent model	DSPC, DSPE-PEG2000, DC-CHOL C_3F_8	galectin-7 siRNA	1 MHz 2 W/cm^{-2} 50% duty 2 min	Significant reductions in inflammatory infiltration and myocyte damage. Prevented acute cellular rejection	Wang et al. [154]
Myocardial I/R (rodent model)	DPPC, DC-CHOL, DSPE-PEG2000 C_3F_6	Short hairpin RNA (shRNA) against PHD2	1 MHz 2 W/cm^{-2} 50% duty 2 min	Reduced infarct size and increased neovascularization	Zhang et al. [155]
Myocardial I/R (rodent model)	HSPC, DOTMA C_3F_8	pDNA AKT	Clinical scanner	Reduced myocardial apoptosis, increased vascular density and better cardiac function	Sun et al. [68]
Myocardial I/R (rodent model)	HSPC, DOTMA, DSPEPEG2000 air	pDNA MMP2 & Timp3	Clinical scanner with second harmonic mode	Improvement in ejection fraction and reduced cardiac scarring	Yan et al. [79]
Acute MI (murine model)	Definity (Lantheus)	pDNA VEGF and SCF	Clinical scanner with mechanical index of 1.6	Increased vascular density, increased ejection fraction and decreased infarct size	Fujii et al. [157]
Acute MI (rabbit model)	DPPA, DSPC, PEG, DSPE-PEG2000, DC-CHOL C_3F_6	pDNA Ang-1, ICAM-1	Clinical scanner with second harmonic mode	Improved angiogenesis and heart function	Zhou et al. [159]

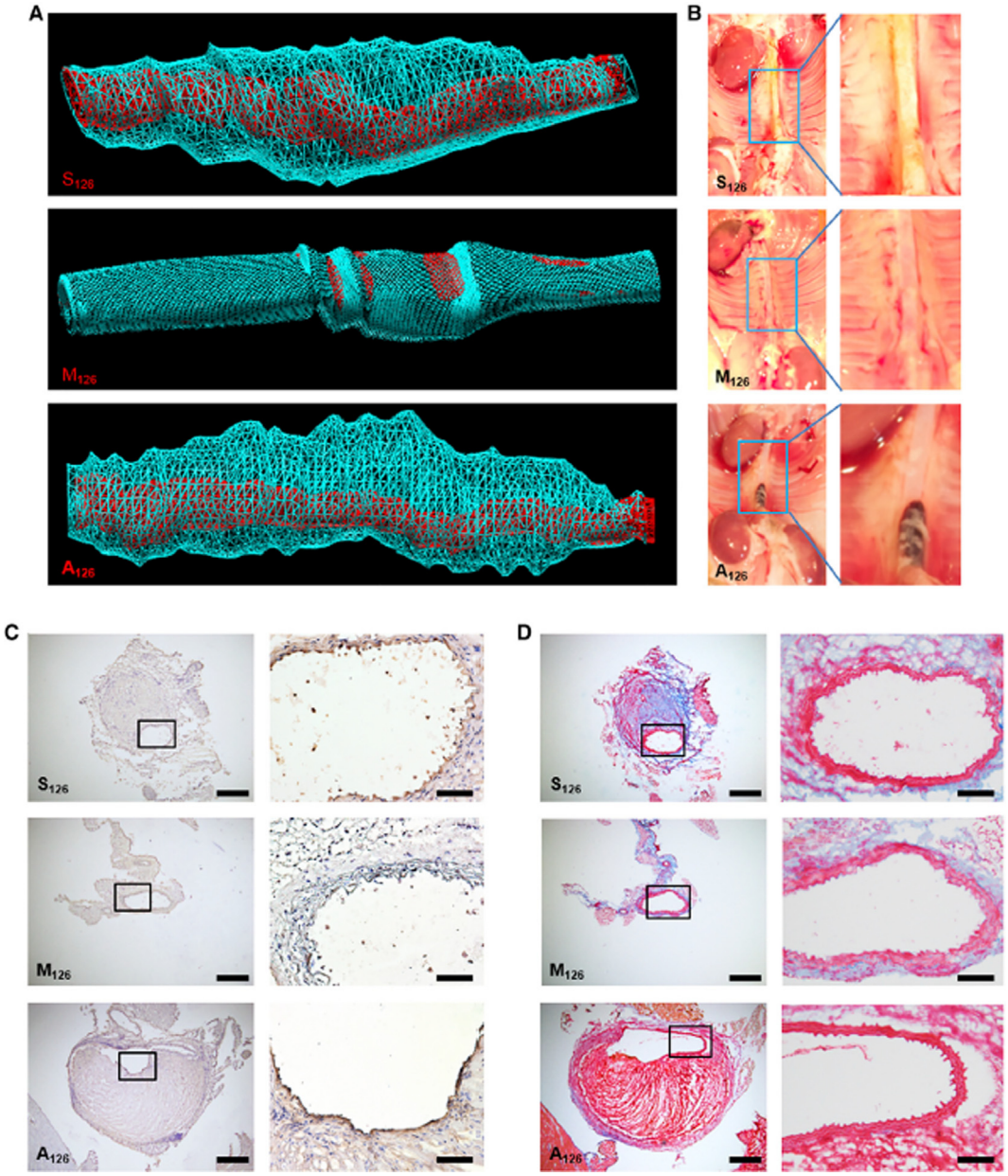

Fig. 6. Representative images of 3D ultrasound reconstructions of abdominal aorta, photographs of vessel isolations, immunohistochemistry, and Martius Scarlet Blue demonstrating profound effect of VCAM-1–targeted miR-carrying microbubbles. **A.** 3D ultrasound reconstruction of abdominal aorta shows vessel lumen (in red), as well as massive areas of plaque build-up and aneurysm (in blue), from animals treated with $Targ^{MB}$-A_{126} or $Targ^{MB}$-S_{126} but not in animals treated with $Targ^{MB}$-M_{126}. **B.** Vessel isolation shows clean abdominal aorta in mice treated with $Targ^{MB}$-M_{126} but plaque build-up and aneurysms in mice given $Targ^{MB}$-S_{126} or $Targ^{MB}$-A_{126}. **C.** Immunohistochemistry confirmed a decrease in VCAM-1 expression for $Targ^{MB}$-M_{126} treated animals as compared to those treated with $Targ^{MB}$-A_{126} or $Targ^{MB}$-S_{126}. **D.** Martius Scarlet Blue showed plaque build-up and aneurysms in abdominal arteries of $Targ^{MB}$-A_{126} or $Targ^{MB}$-S_{126} treated animals, whereas very little plaque build-up was observed in $Targ^{MB}$-M_{126} treated mice [50].

cationic MBs [68]. UTGD therapy with AKT plasmid was performed on day 5 post I/R injury. Outcomes highlighted that their cationic MBs had a higher binding capacity than the commercially available MBs, increased levels of downstream proteins resulting from AKT phosphorylation and activation, reduced myocardial apoptosis, and increased myocardial vascular density, cardiac function, and perfusion [68].

For active targeting, the group further looked at using a matrix metalloproteinase-2 (MMP2) antibody conjugated to cationic MBs to deliver pDNA encoding tissue inhibitor of metalloproteinase (Timp3), a strong inhibitor of MMP2 and matrix metalloproteinase-9 [79]. A single therapy performed 3 days post injury resulted in an improvement in ejection fraction on echocardiography and reduced cardiac scarring on histology at day 21 [79]. In post myocardial I/R injury rabbits, a similar improvement in cardiac function was achieved using active targeting of the intercellular adhesion molecule-1 to deliver pDNA encoding angiopoietin-1 gene into infarcted heart tissue, promoting angiogenesis [159]. The success of these preclinical studies indicates that gene therapy and UTGD can be used for complex cardiovascular diseases. One of the main hurdles for gene therapy in complex diseases is off-target effects. The addition of active targeting to biomarkers will help overcome this limitation; therefore antibody-targeting of other cardiovascular biomarkers [160,161] may further improve the treatment for myocardial I/R injury via UTGD.

Vascular dysfunction is the starting point of atherosclerosis and will ultimately lead to MI, so the ability to reduce vascular inflammation will hinder atherosclerotic progression. In a rabbit model of

iliac artery intimal proliferation, He et al. demonstrated inhibition of smooth muscle cell proliferation and reduced intimal thickness in the animals treated with albumin-based MBs and targeted ultrasound treatment [162]. In an attempt to resist nucleases, He et al. used peptide nucleic acids (PNAs), a DNA analog where the natural nucleic acid's sugar phosphate backbone is replaced by a synthetic peptide backbone [162]. Unlike most other groups, which use the different charges between their carrier and the nucleic acids, the authors directly generated the albumin-based MBs together with PNAs [162].

Three *in vivo* studies investigated UTGD of miR-126, an endothelial-specific miRNA for VCAM-1 [50,163,164]. In an ischemic hindlimb rodent model, UTGD resulted in an improvement in normalized microvascular perfusion [163]. Endo-Takahashi *et al.* have also reported that miR-126-loaded UTGD led to the induction of angiogenic factors and the improvement of blood flow in their ischemic hindlimb murine model [164]. AAA is one of the 10 most common causes of mortality, responsible for 2% of all deaths. AAA is monitored using ultrasound and invasive theory is the only option to prevent a rupture. Wang et al. conjugated single-chain antibody against VCAM-1 onto MBs to achieve targeting of the inflamed endothelium layer on the vessel wall of AAA for dual-targeted delivery of miR-126 [50]. After the targeted MBs were bound to the AAA region, ultrasound bursts were applied to provide UTGD to the abdominal aorta. Using an angiotensin-II infusion murine model of gradual AAA development, the authors showed amelioration of AAA in miR-126 mimic treated animals via 3D ultrasound imaging (Fig. 6) [50]. Further histological data from the study proved downregulation of VCAM-1 expression, as well as successful reduced plaque and aneurysm size [50]. This dual-targeting and site-specific ultrasound trigger may be particularly important for treatments of vascular diseases because the ultrasonic particles will naturally disperse throughout the circulatory system. Overall, preclinical UTGD approaches have shown promising results in gene delivery and potential to provide a targeted medical option for patients.

9. Limitations

Nevertheless, there are some hurdles and considerations before UTGD can be translated to clinical practise. Ultrasound-associated tissue heating with increased frequency has presented a concern and so the frequency and length of imaging should be carefully considered. To further prevent heating, the intensities used are usually between 0.3 and 3 W/cm^2 for drug or gene delivery. Furthermore, an increase in mechanical index, which is the peak negative pressure (MPa), is directly proportional to increased cavitation; therefore the mechanical index typically ranges between 0.2 and 1.9. Some studies have shown that prolonged or repetitive use of ultrasound-targeted MB destruction has been linked to damage to microvasculature integrity, cardiac arrhythmias, and hemolysis [165-170]. While most studies have reported UTGD to be safe, some have also shown tissue damage, especially when subjected to high mechanical indexes [107,108,113]. Ultimately, future research must be conducted, especially in large animals, using human scanners to determine the optimal frequency and intensity of ultrasound. There is also a need to investigate the suitability, toxicology, and circulating half-life of the ultrasonic particles and their efficacy in gene translation. In addition, according to the disease of interest, there is a need to determine the suitable nucleic acids and particle platforms. While a single-gene delivery approach may be suitable for genetic diseases, it may not be as useful in chronic diseases, in particular inflammation and CVDs.

10. Conclusions

The recent successes of LNP platforms for nucleic acid delivery and the high-profile clinical approval of multiple mRNA vaccines for COVID-19 have set the stage for future gene therapy. Research in gene therapy has developed from a delivery of a single gene approach to the site-specific delivery of multiple nucleic acids over repeated treatments. To avoid unnecessary uptake of nanoparticles and nucleic acids, UTGD has been successfully employed to specifically deliver genetic materials to diseased areas across a range of diseases. In particular, this review covers the successful use of UTGD to directly deliver genetic materials to the diseased area, thereby eliminating any off-target effects, for CVDs and cancer. With further advancement in gene therapy, development of ultrasonic particles and improvement in ultrasound technology, the potential for clinical translation of UTGD will benefit patients across a broad spectrum of diseases.

Declaration of Competing Interest

The authors declare that they have no known competing financial interests or personal relationships that could have appeared to influence the work reported in this paper.

Acknowledgments

AW is supported by Monash University Scholarships and a Baker Bright Sparks Scholarship. KP is supported by the Australian National Health and Medical Research Council Investigator L3 Fellowship (GNT1174098). XW is supported by a National Heart Foundation Future Leader Fellowship (101932) and a Baker Fellowship. Some figures were constructed with and modified from Servier Medical Art templates.

References

[1] B.C. Reinhardt, O. Habib, K.L. Shaw, E.K. Garabedian, D.A. Carbonaro-Sarracino, D.R. Terrazas, B. Campo-Fernandez, S. De Oliveira, T.B. Moore, A. Ikeda, B.C. Engel, G.M. Podsakoff, R.P. Hollis, A. Fernandes, C.R. Jackson, S.A. Shupien, S. Mishra, A. Davila, J. Mottahedeh, A. Vitomirov, W. Meng, A.M. Rosenfeld, A.M. Roche, P. Hokama, S. Reddy, J.K. Everett, X. Wang, E.T. Luning Prak, K. Cornetta, M. Hershfield, R. Sokolic, S.S. De Ravin, H.L. Malech, F.D. Bushman, F. Candotti, D.B. Kohn, Long-term Outcomes after Gene Therapy for Adenosine Deaminase Severe Combined Immune Deficiency (ADA SCID), Blood. (2021), https://doi.org/10.1182/blood.2020010260.

[2] L.A. Kohn, D.B. Kohn, Gene Therapies for Primary Immune Deficiencies, Front Immunol. 12 (2021), https://doi.org/10.3389/fimmu.2021.648951 648951.

[3] , Nature Medicine. 27 (2021), https://doi.org/10.1038/s41591-021-01333-6, 563 563.

[4] D.A. Kuzmin, M.V. Shutova, N.R. Johnston, O.P. Smith, V.V. Fedorin, Y.S. Kukushkin, J.C.M. van der Loo, E.C. Johnstone, The clinical landscape for AAV gene therapies, Nature Reviews Drug Discovery. 20 (3) (2021) 173–174, https://doi.org/10.1038/d41573-021-00017-7.

[5] K.S. Corbett, B. Flynn, K.E. Foulds, J.R. Francica, S. Boyoglu-Barnum, A.P. Werner, B. Flach, S. O'Connell, K.W. Bock, M. Minai, B.M. Nagata, H. Andersen, D.R. Martinez, A.T. Noe, N. Douek, M.M. Donaldson, N.N. Nji, G.S. Alvarado, D. K. Edwards, D.R. Flebbe, E. Lamb, N.A. Doria-Rose, B.C. Lin, M.K. Louder, S. O'Dell, S.D. Schmidt, E. Phung, L.A. Chang, C. Yap, J.-P.-M. Todd, L. Pessaint, A. Van Ry, S. Browne, J. Greenhouse, T. Putman-Taylor, A. Strasbaugh, T.-A. Campbell, A. Cook, A. Dodson, K. Steingrebe, W. Shi, Y. Zhang, O.M. Abiona, L. Wang, A. Pegu, E.S. Yang, K. Leung, T. Zhou, I.-T. Teng, A. Widge, I. Gordon, L. Novik, R.A. Gillespie, R.J. Loomis, J.I. Moliva, G. Stewart-Jones, S. Himansu, W.-P. Kong, M.C. Nason, K.M. Morabito, T.J. Ruckwardt, J.E. Ledgerwood, M.R. Gaudinski, P.D. Kwong, J.R. Mascola, A. Carfi, M.G. Lewis, R.S. Baric, A. McDermott, I.N. Moore, N.J. Sullivan, M. Roederer, R.A. Seder, B.S. Graham, Evaluation of the mRNA-1273 Vaccine against SARS-CoV-2 in Nonhuman Primates, N Engl J Med. (2020), https://doi.org/10.1056/NEJMoa2024671.

[6] L.A. Jackson, E.J. Anderson, N.G. Rouphael, P.C. Roberts, M. Makhene, R.N. Coler, M.P. McCullough, J.D. Chappell, M.R. Denison, L.J. Stevens, A.J. Pruijssers, A. McDermott, B. Flach, N.A. Doria-Rose, K.S. Corbett, K.M. Morabito, S. O'Dell, S.D. Schmidt, P.A. Swanson, M. Padilla, J.R. Mascola, K. M. Neuzil, H. Bennett, W. Sun, E. Peters, M. Makowski, J. Albert, K. Cross, W. Buchanan, R. Pikaart-Tautges, J.E. Ledgerwood, B.S. Graham, J.H. Beigel, An mRNA Vaccine against SARS-CoV-2 — Preliminary Report, N Engl J Med. (2020), https://doi.org/10.1056/NEJMoa2022483.

[7] L.R. Baden, H.M. El Sahly, B. Essink, K. Kotloff, S. Frey, R. Novak, D. Diemert, S. A. Spector, N. Rouphael, C.B. Creech, J. McGettigan, S. Kehtan, N. Segall, J. Solis, A. Brosz, C. Fierro, H. Schwartz, K. Neuzil, L. Corey, P. Gilbert, H. Janes, D. Follmann, M. Marovich, J. Mascola, L. Polakowski, J. Ledgerwood, B.S. Graham, H. Bennett, R. Pajon, C. Knightly, B. Leav, W. Deng, H. Zhou, S. Han, M. Ivarsson, J. Miller, T. Zaks, COVE Study Group, Efficacy and Safety of the mRNA-1273 SARS-CoV-2 Vaccine, N Engl J Med. (2020), https://doi.org/10.1056/NEJMoa2035389.

[8] F.P. Polack, S.J. Thomas, N. Kitchin, J. Absalon, A. Gurtman, S. Lockhart, J.L. Perez, G. Pérez Marc, E.D. Moreira, C. Zerbini, R. Bailey, K.A. Swanson, S. Roychoudhury, K. Koury, P. Li, W.V. Kalina, D. Cooper, R.W. Frenck, L.L. Hammitt, Ö. Türeci, H. Nell, A. Schaefer, S. Ünal, D.B. Tresnan, S. Mather, P.R. Dormitzer, U. Şahin, K.U. Jansen, W.C. Gruber, C4591001 Clinical Trial Group, Safety and Efficacy of the BNT162b2 mRNA Covid-19 Vaccine, N Engl J Med. 383 (27) (2020) 2603–2615, https://doi.org/10.1056/NEJMoa2034577.

[9] C. Baum, O. Kustikova, U. Modlich, Z. Li, B. Fehse, Mutagenesis and oncogenesis by chromosomal insertion of gene transfer vectors, Hum Gene Ther. 17 (3) (2006) 253–263, https://doi.org/10.1089/hum.2006.17.253.

[10] N. Bessis, F.J. GarciaCozar, M.-C. Boissier, Immune responses to gene therapy vectors: influence on vector function and effector mechanisms, Gene Ther. 11 (Suppl 1) (2004) S10–S17, https://doi.org/10.1038/sj.gt.3302364.

[11] D. Bouard, D. Alazard-Dany, F.-L. Cosset, Viral vectors: from virology to transgene expression, Br J Pharmacol. 157 (2009) 153–165, https://doi.org/10.1038/bjp.2008.349.

[12] H. Yin, R.L. Kanasty, A.A. Eltoukhy, A.J. Vegas, J.R. Dorkin, D.G. Anderson, Non-viral vectors for gene-based therapy, Nat Rev Genet. 15 (8) (2014) 541–555, https://doi.org/10.1038/nrg3763.

[13] C.E. Thomas, A. Ehrhardt, M.A. Kay, Progress and problems with the use of viral vectors for gene therapy, Nat Rev Genet. 4 (5) (2003) 346–358, https://doi.org/10.1038/nrg1066.

[14] M.-K. Abraham, K. Peter, T. Michel, H.P. Wendel, S. Krajewski, X. Wang, Nanoliposomes for Safe and Efficient Therapeutic mRNA Delivery: A Step Toward Nanotheranostics in Inflammatory and Cardiovascular Diseases as well as Cancer, Nanotheranostics. 1 (2017) 154–165, https://doi.org/10.7150/ntno.19449.

[15] T. Michel, D. Luft, M.-K. Abraham, S. Reinhardt, M.L. Salinas Medina, J. Kurz, M. Schaller, M. Avci-Adali, C. Schlensak, K. Peter, H.P. Wendel, X. Wang, S. Krajewski, Cationic Nanoliposomes Meet mRNA: Efficient Delivery of Modified mRNA Using Hemocompatible and Stable Vectors for Therapeutic Applications, Molecular Therapy - Nucleic Acids. 8 (2017) 459–468, https://doi.org/10.1016/j.omtn.2017.07.013.

[16] T. Coelho, D. Adams, A. Silva, P. Lozeron, P.N. Hawkins, T. Mant, J. Perez, J. Chiesa, S. Warrington, E. Tranter, M. Munisamy, R. Falzone, J. Harrop, J. Cehelsky, B.R. Bettencourt, M. Geissler, J.S. Butler, A. Sehgal, R.E. Meyers, Q. Chen, T. Borland, R.M. Hutabarat, V.A. Clausen, R. Alvarez, K. Fitzgerald, C. Gamba-Vitalo, S.V. Nochur, A.K. Vaishnaw, D.W.Y. Sah, J.A. Gollob, O.B. Suhr, Safety and efficacy of RNAi therapy for transthyretin amyloidosis, N Engl J Med. 369 (9) (2013) 819–829, https://doi.org/10.1056/NEJMoa1208760.

[17] A. Khurana, P. Allawadhi, I. Khurana, S. Allwadhi, R. Weiskirchen, A.K. Banothu, D. Chhabra, K. Joshi, K.K. Bharani, Role of nanotechnology behind the success of mRNA vaccines for COVID-19, Nano Today. 38 (2021), https://doi.org/10.1016/j.nantod.2021.101142 101142.

[18] M.S. Shim, Y.J. Kwon, Stimuli-responsive polymers and nanomaterials for gene delivery and imaging applications, Adv Drug Deliv Rev. 64 (11) (2012) 1046–1059, https://doi.org/10.1016/j.addr.2012.01.018.

[19] A. D'Andrea, S. Sperlongano, M. Pacileo, E. Venturini, G. Iannuzzo, M. Gentile, R. Sperlongano, G. Vitale, M. Maglione, G. Cice, F. Maria Sarullo, A. Di Lorenzo, C. Vigorito, F. Giallauria, E. Picano, New Ultrasound Technologies for Ischemic Heart Disease Assessment and Monitoring in Cardiac Rehabilitation, J Clin Med. 9 (2020), https://doi.org/10.3390/jcm9103131.

[20] Y. Yoshii, C. Zhao, P.C. Amadio, Recent Advances in Ultrasound Diagnosis of Carpal Tunnel Syndrome, Diagnostics (Basel). 10 (2020), https://doi.org/10.3390/diagnostics10080596.

[21] A. Boussuges, S. Rives, J. Finance, F. Brégeon, Assessment of diaphragmatic function by ultrasonography: Current approach and perspectives, World J Clin Cases. 8 (2020) 2408–2424. 10.12998/wjcc.v8.i12.2408.

[22] F.Y. Rizi, J. Au, H. Yli-Ollila, S. Golemati, M. Makūnaitė, M. Orkisz, N. Navab, M. MacDonald, T.M. Laitinen, H. Behnam, Z. Gao, A. Gastounioti, R. Jurkonis, D. Vray, T. Laitinen, A. Sérusclat, K.S. Nikita, G. Zahnd, Carotid Wall Longitudinal Motion in Ultrasound Imaging: An Expert Consensus Review, Ultrasound Med Biol. 46 (10) (2020) 2605–2624, https://doi.org/10.1016/j.ultrasmedbio.2020.06.006.

[23] N.N. Khanna, A.D. Jamthikar, D. Gupta, M. Piga, L. Saba, C. Carcassi, A.A. Giannopoulos, A. Nicolaides, J.R. Laird, H.S. Suri, S. Mavrogeni, A.D. Protogerou, P. Sfikakis, G.D. Kitas, J.S. Suri, Rheumatoid Arthritis: Atherosclerosis Imaging and Cardiovascular Risk Assessment Using Machine and Deep Learning-Based Tissue Characterization, Curr Atheroscler Rep. 21 (2019) 7, https://doi.org/10.1007/s11883-019-0766-x.

[24] Z. Akkus, J. Cai, A. Boonrod, A. Zeinoddini, A.D. Weston, K.A. Philbrick, B.J. Erickson, A Survey of Deep-Learning Applications in Ultrasound: Artificial Intelligence-Powered Ultrasound for Improving Clinical Workflow, J Am Coll Radiol. 16 (2019) 1318–1328, https://doi.org/10.1016/j.jacr.2019.06.004.

[25] K. Shung, J. Cannata, M. Qifa Zhou, J. Lee, High frequency ultrasound: a new frontier for ultrasound, Annu Int Conf IEEE Eng Med, Biol Soc. (2009 (2009) 1953–1955.), https://doi.org/10.1109/IEMBS.2009.5333463.

[26] G.R. Lockwood, D.H. Turnball, D.A. Christopher, F.S. Foster, Beyond 30 MHz [applications of high-frequency ultrasound imaging], IEEE Engineering in Medicine and Biology Magazine. 15 (1996) 60–71, https://doi.org/10.1109/51.544513.

[27] X. Wang, C.E. Hagemeyer, J.D. Hohmann, E. Leitner, P.C. Armstrong, F. Jia, M. Olschewski, A. Needles, K. Peter, I. Ahrens, Novel Single-Chain Antibody-Targeted Microbubbles for Molecular Ultrasound Imaging of Thrombosis: Validation of a Unique Noninvasive Method for Rapid and Sensitive Detection of Thrombi and Monitoring of Success or Failure of Thrombolysis in Mice, Circulation. 125 (2012) 3117–3126, https://doi.org/10.1161/CIRCULATIONAHA.111.030312.

[28] X. Wang, J. Palasubramaniam, Y. Gkanatsas, J.D. Hohmann, E. Westein, R. Kanojia, K. Alt, D. Huang, F. Jia, I. Ahrens, R.L. Medcalf, K. Peter, C.E. Hagemeyer, Towards effective and safe thrombolysis and thromboprophylaxis: preclinical testing of a novel antibody-targeted recombinant plasminogen activator directed against activated platelets, Circ. Res. 114 (2014) 1083–1093, https://doi.org/10.1161/CIRCRESAHA.114.302514.

[29] X. Wang, Y. Gkanatsas, J. Palasubramaniam, J.D. Hohmann, Y.C. Chen, B. Lim, C. Hagemeyer, K. Peter, Thrombus-Targeted Theranostic Microbubbles: A New Technology towards Concurrent Rapid Ultrasound Diagnosis and Bleeding-free Fibrinolytic Treatment of Thrombosis, Theranostics. 6 (2016) 726–738.

[30] L. Sun, C.-L. Lien, X. Xu, K.K. Shung, In vivo cardiac imaging of adult zebrafish using high frequency ultrasound (45–75 MHz), Ultrasound Med Biol. 34 (1) (2008) 31–39, https://doi.org/10.1016/j.ultrasmedbio.2007.07.002.

[31] L.W. Wang, I.G. Huttner, C.F. Santiago, S.H. Kesteven, Z.-Y. Yu, M.P. Feneley, D. Fatkin, Standardized echocardiographic assessment of cardiac function in normal adult zebrafish and heart disease models, Dis Model Mech. 10 (2017) 63–76, https://doi.org/10.1242/dmm.026989.

[32] P.A. Dayton, J.J. Rychak, Molecular ultrasound imaging using microbubble contrast agents, Front Biosci. 12 (2007) 5124–5142, https://doi.org/10.2741/2553.

[33] J.-U. Voigt, Ultrasound molecular imaging, Methods. 48 (2) (2009) 92–97, https://doi.org/10.1016/j.ymeth.2009.03.011.

[34] R. Gessner, P.A. Dayton, Advances in molecular imaging with ultrasound 7290.2010.00022 Mol Imaging. 9 (3) (2010), https://doi.org/10.2310/7290.2010.00022.

[35] J.M. Correas, L. Bridal, A. Lesavre, A. Méjean, M. Claudon, O. Hélénon, Ultrasound contrast agents: properties, principles of action, tolerance, and artifacts, Eur Radiol. 11 (2001) 1316–1328, https://doi.org/10.1007/s003300100940.

[36] A.L. Klibanov, Microbubble contrast agents: targeted ultrasound imaging and ultrasound-assisted drug-delivery applications, Invest Radiol. 41 (2006) 354–362, https://doi.org/10.1097/01.rli.0000199292.88189.0f.

[37] K. Kooiman, S. Roovers, S.A.G. Langeveld, R.T. Kleven, H. Dewitte, M.A. O'Reilly, J.-M. Escoffre, A. Bouakaz, M.D. Verweij, K. Hynynen, I. Lentacker, E. Stride, C.K. Holland, Ultrasound-Responsive Cavitation Nuclei for Therapy and Drug Delivery, Ultrasound Med Biol. 46 (6) (2020) 1296–1325, https://doi.org/10.1016/j.ultrasmedbio.2020.01.002.

[38] I. Lentacker, I. De Cock, R. Deckers, S.C. De Smedt, C.T.W. Moonen, Understanding ultrasound induced sonoporation: definitions and underlying mechanisms, Adv Drug Deliv Rev. 72 (2014) 49–64, https://doi.org/10.1016/j.addr.2013.11.008.

[39] B. Geers, H. Dewitte, S.C. De Smedt, I. Lentacker, Crucial factors and emerging concepts in ultrasound-triggered drug delivery, J Control Release. 164 (3) (2012) 248–255, https://doi.org/10.1016/j.jconrel.2012.08.014.

[40] Ý. Mørch, R. Hansen, S. Berg, A.K.O. Åslund, W.R. Glomm, S. Eggen, R. Schmid, H. Johnsen, S. Kubowicz, S. Snipstad, E. Sulheim, S. Hak, G. Singh, B.H. McDonagh, H. Blom, C. de Lange Davies, P.M. Stenstad, Nanoparticle-stabilized microbubbles for multimodal imaging and drug delivery, Contrast Media Mol Imaging. 10 (5) (2015) 356–366, https://doi.org/10.1002/cmmi.v10.510.1002/cmmi.1639.

[41] A.L. Klibanov, Ligand-carrying gas-filled microbubbles: ultrasound contrast agents for targeted molecular imaging, Bioconjug Chem. 16 (2005) 9–17, https://doi.org/10.1021/bc049898y.

[42] A. Bouakaz, N. de Jong, C. Cachard, K. Jouini, On the effect of lung filtering and cardiac pressure on the standard properties of ultrasound contrast agent, Ultrasonics. 36 (1-5) (1998) 703–708, https://doi.org/10.1016/S0041-624X(97)00137-6.

[43] B.A. Kaufmann, J.R. Lindner, Molecular imaging with targeted contrast ultrasound, Curr Opin Biotechnol. 18 (1) (2007) 11–16, https://doi.org/10.1016/j.copbio.2007.01.004.

[44] S.L. Mulvagh, H. Rakowski, M.A. Vannan, S.S. Abdelmoneim, H. Becher, S.M. Bierig, P.N. Burns, R. Castello, P.D. Coon, M.E. Hagen, J.G. Jollis, T.R. Kimball, D. W. Kitzman, I. Kronzon, A.J. Labovitz, R.M. Lang, J. Mathew, W.S. Moir, S.F. Nagueh, A.S. Pearlman, J.E. Perez, T.R. Porter, J. Rosenbloom, G.M. Strachan, S. Thanigaraj, K. Wei, A. Woo, E.H.C. Yu, W.A. Zoghbi, American Society of Echocardiography Consensus Statement on the Clinical Applications of Ultrasonic Contrast Agents in Echocardiography, Journal of the American Society of Echocardiography. 21 (11) (2008) 1179–1201, https://doi.org/10.1016/j.echo.2008.09.009.

[45] R. Senior, H. Becher, M. Monaghan, L. Agati, J. Zamorano, J.L. Vanoverschelde, P. Nihoyannopoulos, Contrast echocardiography: evidence-based recommendations by European Association of Echocardiography, Eur J Echocardiogr. 10 (2009) 194–212, https://doi.org/10.1093/ejechocard/jep005.

[46] X. Wang, K. Peter, Molecular Imaging of Atherothrombotic Diseases: Seeing Is Believing, Arterioscler. Thromb. Vasc. Biol. 37 (6) (2017) 1029–1040, https://doi.org/10.1161/ATVBAHA.116.306483.
[47] J. Guo, X. Wang, D.C. Henstridge, J.J. Richardson, J. Cui, A. Sharma, M.A. Febbraio, K. Peter, J.B. de Haan, C.E. Hagemeyer, F. Caruso, Nanoporous Metal-Phenolic Particles as Ultrasound Imaging Probes for Hydrogen Peroxide, Adv Healthc Mater. 4 (14) (2015) 2170–2175, https://doi.org/10.1002/adhm.201500528.
[48] J.-T. Walker, X. Wang, K. Peter, K. Kempe, S.R. Corrie, Dynamic Solid-State Ultrasound Contrast Agent for Monitoring pH Fluctuations In Vivo, ACS Sens. 5 (4) (2020) 1190–1197, https://doi.org/10.1021/acssensors.0c0024510.1021/acssensors.0c00245.s001.
[49] J.J. Rychak, A.L. Klibanov, Nucleic acid delivery with microbubbles and ultrasound, Adv Drug Deliv Rev. 72 (2014) 82–93, https://doi.org/10.1016/j.addr.2014.01.009.
[50] X. Wang, A.K. Searle, J.D. Hohmann, A.L. Liu, M.-K. Abraham, J. Palasubramaniam, B. Lim, Y.u. Yao, M. Wallert, E. Yu, Y.-C. Chen, K. Peter, Dual-Targeted Theranostic Delivery of miRs Arrests Abdominal Aortic Aneurysm Development, Mol. Ther. 26 (4) (2018) 1056–1065, https://doi.org/10.1016/j.ymthe.2018.02.010.
[51] J. Deprez, G. Lajoinie, Y. Engelen, S.C. De Smedt, I. Lentacker, Opening doors with ultrasound and microbubbles: Beating biological barriers to promote drug delivery, Adv Drug Deliv Rev. 172 (2021) 9–36, https://doi.org/10.1016/j.addr.2021.02.015.
[52] F.S. Villanueva, W.R. Wagner, Ultrasound molecular imaging of cardiovascular disease, Nat Clin Pract Cardiovasc Med. 5 (Suppl 2) (2008) S26–S32, https://doi.org/10.1038/ncpcardio1246.
[53] C.-H. Fan, C.-Y. Lin, H.-L. Liu, C.-K. Yeh, Ultrasound targeted CNS gene delivery for Parkinson's disease treatment, J Control Release. 261 (2017) 246–262, https://doi.org/10.1016/j.jconrel.2017.07.004.
[54] I. De Cock, G. Lajoinie, M. Versluis, S.C. De Smedt, I. Lentacker, Sonoprinting and the importance of microbubble loading for the ultrasound mediated cellular delivery of nanoparticles, Biomaterials. 83 (2016) 294–307, https://doi.org/10.1016/j.biomaterials.2016.01.022.
[55] S. Zullino, M. Argenziano, I. Stura, C. Guiot, R. Cavalli, From Micro- to Nano-Multifunctional Theranostic Platform: Effective Ultrasound Imaging Is Not Just a Matter of Scale, Molecular Imaging. 17 (2018), https://doi.org/10.1177/1536012118778216.
[56] S.R. Sirsi, M.A. Borden, Advances in ultrasound mediated gene therapy using microbubble contrast agents, Theranostics. 2 (12) (2012) 1208–1222, https://doi.org/10.7150/thno.4306.
[57] J. Wu, R.-K. Li, Ultrasound-targeted microbubble destruction in gene therapy: A new tool to cure human diseases, Genes Dis. 4 (2017) 64–74, https://doi.org/10.1016/j.gendis.2016.08.001.
[58] Y. Endo-Takahashi, Y. Negishi, Microbubbles and Nanobubbles with Ultrasound for Systemic Gene Delivery, Pharmaceutics. 12 (2020), https://doi.org/10.3390/pharmaceutics12100964.
[59] A. Presset, C. Bonneau, S. Kazuyoshi, L. Nadal-Desbarats, T. Mitsuyoshi, A. Bouakaz, N. Kudo, J.-M. Escoffre, N. Sasaki, Endothelial Cells, First Target of Drug Delivery Using Microbubble-Assisted Ultrasound, Ultrasound Med Biol. 46 (7) (2020) 1565–1583, https://doi.org/10.1016/j.ultrasmedbio.2020.03.013.
[60] M.L. Yap, J.D. McFadyen, X. Wang, N.A. Zia, J.D. Hohmann, M. Ziegler, Y. Yao, A. Pham, M. Harris, P.S. Donnelly, P.M. Hogarth, G.A. Pietersz, B. Lim, K. Peter, Targeting Activated Platelets: A Unique and Potentially Universal Approach for Cancer Imaging, Theranostics. 7 (2017) 2565–2574, https://doi.org/10.7150/thno.19900.
[61] S.M. Chowdhury, L. Abou-Elkacem, T. Lee, J. Dahl, A.M. Lutz, Ultrasound and microbubble mediated therapeutic delivery: Underlying mechanisms and future outlook, J Control Release. 326 (2020) 75–90, https://doi.org/10.1016/j.jconrel.2020.06.008.
[62] K.-C. Tsai, Z.-K. Liao, S.-J. Yang, W.-L. Lin, M.-J. Shieh, L.-H. Hwang, W.-S. Chen, Differences in gene expression between sonoporation in tumor and in muscle, J Gene Med. 11 (10) (2009) 933–940, https://doi.org/10.1002/jgm.v11:1010.1002/jgm.1376.
[63] Y. Xiao, K. Shi, Y. Qu, B. Chu, Z. Qian, Engineering Nanoparticles for Targeted Delivery of Nucleic Acid Therapeutics in Tumor, Molecular Therapy - Methods & Clinical Development. 12 (2019) 1–18, https://doi.org/10.1016/j.omtm.2018.09.002.
[64] A. Wadhwa, A. Aljabbari, A. Lokras, C. Foged, A. Thakur, Opportunities and Challenges in the Delivery of mRNA-Based Vaccines, Pharmaceutics. 12 (2020) 102, https://doi.org/10.3390/pharmaceutics12020102.
[65] E. Mastrobattista, M.A.E.M. van der Aa, W.E. Hennink, D.J.A. Crommelin, Artificial viruses: a nanotechnological approach to gene delivery, Nat Rev Drug Discov. 5 (2) (2006) 115–121, https://doi.org/10.1038/nrd1960.
[66] J.P. Christiansen, B.A. French, A.L. Klibanov, S. Kaul, J.R. Lindner, Targeted tissue transfection with ultrasound destruction of plasmid-bearing cationic microbubbles, Ultrasound Med Biol. 29 (12) (2003) 1759–1767, https://doi.org/10.1016/S0301-5629(03)00976-1.
[67] C.M. Panje, D.S. Wang, M.A. Pysz, R. Paulmurugan, Y. Ren, F. Tranquart, L. Tian, J.K. Willmann, Ultrasound-mediated gene delivery with cationic versus neutral microbubbles: effect of DNA and microbubble dose on in vivo transfection efficiency, Theranostics. 2 (2012) 1078–1091, https://doi.org/10.7150/thno.4240.
[68] L.u. Sun, C.-W. Huang, J. Wu, K.-J. Chen, S.-H. Li, R.D. Weisel, H. Rakowski, H.-W. Sung, R.-K. Li, The use of cationic microbubbles to improve ultrasound-targeted gene delivery to the ischemic myocardium, Biomaterials. 34 (8) (2013) 2107–2116, https://doi.org/10.1016/j.biomaterials.2012.11.041.
[69] C. Wan, J. Qian, F. Li, H. Li, Ultrasound-targeted microbubble destruction enhances polyethylenimine-mediated gene transfection *in vitro* in human retinal pigment epithelial cells and in vivo in rat retina, Mol Med Rep. 12 (2015) 2835–2841, https://doi.org/10.3892/mmr.2015.3703.
[70] S.R. Sirsi, S.L. Hernandez, L. Zielinski, H. Blomback, A. Koubaa, M. Synder, S. Homma, J.J. Kandel, D.J. Yamashiro, M.A. Borden, Polyplex-microbubble hybrids for ultrasound-guided plasmid DNA delivery to solid tumors, J Control Release. 157 (2) (2012) 224–234, https://doi.org/10.1016/j.jconrel.2011.09.071.
[71] P. Wang, T. Yin, J. Li, B. Zheng, X. Wang, Y. Wang, J. Zheng, R. Zheng, X. Shuai, Ultrasound-responsive microbubbles for sonography-guided siRNA delivery, Nanomedicine. 12 (4) (2016) 1139–1149, https://doi.org/10.1016/j.nano.2015.12.361.
[72] Y.-P. Xiao, J. Zhang, Y.-H. Liu, J.-H. Zhang, Q.-Y. Yu, Z. Huang, X.-Q. Yu, Low molecular weight PEI-based fluorinated polymers for efficient gene delivery, Eur J Med Chem. 162 (2019) 602–611, https://doi.org/10.1016/j.ejmech.2018.11.041.
[73] Y.-P. Xiao, J.i. Zhang, Y.-H. Liu, Z. Huang, B. Wang, Y.-M. Zhang, X.-Q. Yu, Cross-linked polymers with fluorinated bridges for efficient gene delivery, J Mater Chem B. 5 (43) (2017) 8542–8553, https://doi.org/10.1039/C7TB02158E.
[74] J. Zabner, A.J. Fasbender, T. Moninger, K.A. Poellinger, M.J. Welsh, Cellular and molecular barriers to gene transfer by a cationic lipid, J Biol Chem. 270 (32) (1995) 18997–19007, https://doi.org/10.1074/jbc.270.32.18997.
[75] D.S. Wang, C. Panje, M.A. Pysz, R. Paulmurugan, J. Rosenberg, S.S. Gambhir, M. Schneider, J.K. Willmann, Cationic versus neutral microbubbles for ultrasound-mediated gene delivery in cancer, Radiology. 264 (3) (2012) 721–732, https://doi.org/10.1148/radiol.12112368.
[76] Y.u. Zhou, H. Gu, Y. Xu, F. Li, S. Kuang, Z. Wang, X. Zhou, H. Ma, P. Li, Y. Zheng, H. Ran, J. Jian, Y. Zhao, W. Song, Q. Wang, D. Wang, Targeted antiangiogenesis gene therapy using targeted cationic microbubbles conjugated with CD105 antibody compared with untargeted cationic and neutral microbubbles, Theranostics. 5 (4) (2015) 399–417, https://doi.org/10.7150/thno.10351.
[77] Y. Endo-Takahashi, Y. Negishi, Y. Kato, R. Suzuki, K. Maruyama, Y. Aramaki, Efficient siRNA delivery using novel siRNA-loaded Bubble liposomes and ultrasound, Int J Pharm. 422 (1-2) (2012) 504–509, https://doi.org/10.1016/j.ijpharm.2011.11.023.
[78] L. Yi, Y. Chen, Q. Jin, C. Deng, Y. Wu, H. Li, T. Liu, Y. Li, Y. Yang, J. Wang, Q. Lv, L. Zhang, M. Xie, Antagomir-155 Attenuates Acute Cardiac Rejection Using Ultrasound Targeted Microbubbles Destruction, Adv Healthc Mater. 9 (2020), https://doi.org/10.1002/adhm.202000189 e2000189.
[79] P. Yan, K.-J. Chen, J. Wu, L.u. Sun, H.-W. Sung, R.D. Weisel, J. Xie, R.-K. Li, The use of MMP2 antibody-conjugated cationic microbubble to target the ischemic myocardium, enhance Timp3 gene transfection and improve cardiac function, Biomaterials. 35 (3) (2014) 1063–1073, https://doi.org/10.1016/j.biomaterials.2013.10.043.
[80] X. Hou, T. Zaks, R. Langer, Y. Dong, Lipid nanoparticles for mRNA delivery, Nat Rev Mater. (2021) 1–17, https://doi.org/10.1038/s41578-021-00358-0.
[81] A. Akinc, M.A. Maier, M. Manoharan, K. Fitzgerald, M. Jayaraman, S. Barros, S. Ansell, X. Du, M.J. Hope, T.D. Madden, B.L. Mui, S.C. Semple, Y.K. Tam, M. Ciufolini, D. Witzigmann, J.A. Kulkarni, R. van der Meel, P.R. Cullis, The Onpattro story and the clinical translation of nanomedicines containing nucleic acid-based drugs, Nat Nanotechnol. 14 (12) (2019) 1084–1087, https://doi.org/10.1038/s41565-019-0591-y.
[82] O. Andries, M.D. Filette, S.C. De Smedt, J.o. Demeester, M.V. Poucke, L. Peelman, N.N. Sanders, Innate immune response and programmed cell death following carrier-mediated delivery of unmodified mRNA to respiratory cells, J Control Release. 167 (2) (2013) 157–166, https://doi.org/10.1016/j.jconrel.2013.01.033.
[83] Q.L. Lu, H.-D. Liang, T. Partridge, M.J.K. Blomley, Microbubble ultrasound improves the efficiency of gene transduction in skeletal muscle in vivo with reduced tissue damage, Gene Ther. 10 (5) (2003) 396–405, https://doi.org/10.1038/sj.gt.3301913.
[84] S. Sonoda, K. Tachibana, T. Yamashita, M. Shirasawa, H. Terasaki, E. Uchino, R. Suzuki, K. Maruyama, T. Sakamoto, Selective gene transfer to the retina using intravitreal ultrasound irradiation, J Ophthalmol. 2012 (2012), https://doi.org/10.1155/2012/412752 412752.
[85] B. Tayier, Z. Deng, Y.u. Wang, W. Wang, Y. Mu, F. Yan, Biosynthetic nanobubbles for targeted gene delivery by focused ultrasound, Nanoscale. 11 (31) (2019) 14757–14768, https://doi.org/10.1039/C9NR03402A.
[86] X. Wang, D. Niu, C. Hu, P. Li, Polyethyleneimine-Based Nanocarriers for Gene Delivery, Curr Pharm Des. 21 (2015) 6140–6156, https://doi.org/10.2174/1381612821666151027152907.
[87] G. Chen, K. Wang, P. Wu, Y. Wang, Z. Zhou, L. Yin, M. Sun, D. Oupický, Development of fluorinated polyplex nanoemulsions for improved small interfering RNA delivery and cancer therapy, Nano Res. 11 (7) (2018) 3746–3761, https://doi.org/10.1007/s12274-017-1946-z.
[88] R. Tenchov, R. Bird, A.E. Curtze, Q. Zhou, Lipid Nanoparticles—From Liposomes to mRNA Vaccine Delivery, a Landscape of Research Diversity and Advancement, ACS Nano. (2021), https://doi.org/10.1021/acsnano.1c04996.
[89] M.-K. Abraham, A. Nolte, R. Reus, A. Behring, D. Zengerle, M. Avci-Adali, J.D. Hohmann, K. Peter, C. Schlensak, H.P. Wendel, S. Krajewski, *In vitro* Study of a

Novel Stent Coating Using Modified CD39 Messenger RNA to Potentially Reduce Stent Angioplasty-Associated Complications, PLoS ONE. 10 (2015), https://doi.org/10.1371/journal.pone.0138375 e0138375.
[90] A. Dadwal, A. Baldi, R. Kumar Narang, Nanoparticles as carriers for drug delivery in cancer, Artificial Cells, Nanomedicine, and Biotechnology. 46 (2018) 295–305, https://doi.org/10.1080/21691401.2018.1457039.
[91] S. Sabnis, E.S. Kumarasinghe, T. Salerno, C. Mihai, T. Ketova, J.J. Senn, A. Lynn, A. Bulychev, I. McFadyen, J. Chan, Ö. Almarsson, M.G. Stanton, K.E. Benenato, A Novel Amino Lipid Series for mRNA Delivery: Improved Endosomal Escape and Sustained Pharmacology and Safety in Non-human Primates, Mol Ther. 26 (2018) 1509–1519, https://doi.org/10.1016/j.ymthe.2018.03.010.
[92] Z. Du, M.M. Munye, A.D. Tagalakis, M.D.I. Manunta, S.L. Hart, The Role of the Helper Lipid on the DNA Transfection Efficiency of Lipopolyplex Formulations, Sci Rep. 4 (2014) 7107, https://doi.org/10.1038/srep07107.
[93] J. Kim, Y. Eygeris, M. Gupta, G. Sahay, Self-assembled mRNA vaccines, Adv Drug Deliv Rev. 170 (2021) 83–112, https://doi.org/10.1016/j.addr.2020.12.014.
[94] Y. Zhao, L. Huang, Lipid Nanoparticles for Gene Delivery, Adv Genet. 88 (2014) 13–36, https://doi.org/10.1016/B978-0-12-800148-6.00002-X.
[95] S.-D. Li, L. Huang, Stealth nanoparticles: high density but sheddable PEG is a key for tumor targeting, J Control Release. 145 (2010) 178–181, https://doi.org/10.1016/j.jconrel.2010.03.016.
[96] J.S. Suk, Q. Xu, N. Kim, J. Hanes, L.M. Ensign, PEGylation as a strategy for improving nanoparticle-based drug and gene delivery, Adv Drug Deliv Rev. 99 (2016) 28–51, https://doi.org/10.1016/j.addr.2015.09.012.
[97] R. Díaz-López, N. Tsapis, E. Fattal, Liquid perfluorocarbons as contrast agents for ultrasonography and (19)F-MRI, Pharm Res. 27 (1) (2010) 1–16, https://doi.org/10.1007/s11095-009-0001-5.
[98] X. Cai, Y. Jiang, M. Lin, J. Zhang, H. Guo, F. Yang, W. Leung, C. Xu, Ultrasound-Responsive Materials for Drug/Gene Delivery, Front Pharmacol. 10 (2019) 1650, https://doi.org/10.3389/fphar.2019.01650.
[99] D.i. Gao, M. Xu, Z. Cao, J. Gao, Y.a. Chen, Y. Li, Z. Yang, X. Xie, Q. Jiang, W. Wang, J. Liu, Ultrasound-Triggered Phase-Transition Cationic Nanodroplets for Enhanced Gene Delivery, ACS Appl Mater Interfaces. 7 (24) (2015) 13524–13537, https://doi.org/10.1021/acsami.5b02832.
[100] E. Elizondo, E. Moreno, I. Cabrera, A. Córdoba, S. Sala, J. Veciana, N. Ventosa, Liposomes and other vesicular systems: structural characteristics, methods of preparation, and use in nanomedicine, Prog Mol Biol Transl Sci. 104 (2011) 1–52, https://doi.org/10.1016/b978-0-12-416020-0.00001-2.
[101] A. Akbarzadeh, R. Rezaei-Sadabady, S. Davaran, S.W. Joo, N. Zarghami, Y. Hanifehpour, M. Samiei, M. Kouhi, K. Nejati-Koshki, Liposome: classification, preparation, and applications, Nanoscale Res Lett. 8 (2013) 102, https://doi.org/10.1186/1556-276X-8-102.
[102] I. Lentacker, S.C. De Smedt, J. Demeester, V. Van Marck, M. Bracke, N.N. Sanders, Lipoplex-Loaded Microbubbles for Gene Delivery: A Trojan Horse Controlled by Ultrasound, Advanced Functional Materials. 17 (12) (2007) 1910–1916, https://doi.org/10.1002/adfm.v17:1210.1002/adfm.200700106.
[103] R.E. Vandenbroucke, I. Lentacker, J. Demeester, S.C. De Smedt, N.N. Sanders, Ultrasound assisted siRNA delivery using PEG-siPlex loaded microbubbles, J Control Release. 126 (3) (2008) 265–273, https://doi.org/10.1016/j.jconrel.2007.12.001.
[104] M.-L. De Temmerman, H. Dewitte, R.E. Vandenbroucke, B. Lucas, C. Libert, J.o. Demeester, S.C. De Smedt, I. Lentacker, J. Rejman, mRNA-Lipoplex loaded microbubble contrast agents for ultrasound-assisted transfection of dendritic cells, Biomaterials. 32 (34) (2011) 9128–9135, https://doi.org/10.1016/j.biomaterials.2011.08.024.
[105] Y.-C. Chen, H.-D. Liang, Q.-P. Zhang, M.J.K. Blomley, Q.L. Lu, Pluronic block copolymers: novel functions in ultrasound-mediated gene transfer and against cell damage, Ultrasound Med Biol. 32 (2006) 131–137, https://doi.org/10.1016/j.ultrasmedbio.2005.10.002.
[106] H. Yang, L. Deng, T. Li, X. Shen, J. Yan, L. Zuo, C. Wu, Y. Liu, Multifunctional PLGA Nanobubbles as Theranostic Agents: Combining Doxorubicin and P-gp siRNA Co-Delivery Into Human Breast Cancer Cells and Ultrasound Cellular Imaging, J Biomed Nanotechnol. 11 (2015) 2124–2136, https://doi.org/10.1166/jbn.2015.2168.
[107] M.L. Noble, C.S. Kuhr, S.S. Graves, K.R. Loeb, S.S. Sun, G.W. Keilman, K.P. Morrison, M. Paun, R.F. Storb, C.H. Miao, Ultrasound-targeted microbubble destruction-mediated gene delivery into canine livers, Mol Ther. 21 (9) (2013) 1687–1694, https://doi.org/10.1038/mt.2013.107.
[108] S. Manta, G. Renault, A. Delalande, O. Couture, I. Lagoutte, J. Seguin, F. Lager, P. Houzé, P. Midoux, M. Bessodes, D. Scherman, M.-F. Bureau, C. Marie, C. Pichon, N. Mignet, Cationic microbubbles and antibiotic-free miniplasmid for sustained ultrasound-mediated transgene expression in liver, J Control Release. 262 (2017) 170–181, https://doi.org/10.1016/j.jconrel.2017.07.015.
[109] D.M. Tran, J. Harrang, S. Song, J. Chen, B.M. Smith, C.H. Miao, Prolonging pulse duration in ultrasound-mediated gene delivery lowers acoustic pressure threshold for efficient gene transfer to cells and small animals, J Control Release. 279 (2018) 345–354, https://doi.org/10.1016/j.jconrel.2018.04.012.
[110] D.M. Tran, F. Zhang, K.P. Morrison, K.R. Loeb, J. Harrang, M. Kajimoto, F. Chavez, L. Wu, C.H. Miao, Transcutaneous Ultrasound-Mediated Nonviral Gene Delivery to the Liver in a Porcine Model, Mol Ther Methods Clin Dev. 14 (2019) 275–284, https://doi.org/10.1016/j.omtm.2019.07.005.
[111] Z.-Y. Chen, K. Liang, R.-X. Qiu, Targeted gene delivery in tumor xenografts by the combination of ultrasound-targeted microbubble destruction and polyethylenimine to inhibit survivin gene expression and induce apoptosis, J Exp Clin Cancer Res. 29 (2010) 152, https://doi.org/10.1186/1756-9966-29-152.
[112] Z.P. Shen, A.A. Brayman, L. Chen, C.H. Miao, Ultrasound with microbubbles enhances gene expression of plasmid DNA in the liver via intraportal delivery, Gene Ther. 15 (16) (2008) 1147–1155, https://doi.org/10.1038/gt.2008.51.
[113] J. Park, Y. Zhang, N. Vykhodtseva, J.D. Akula, N.J. McDannold, Targeted and Reversible Blood-Retinal Barrier Disruption via Focused Ultrasound and Microbubbles, PLoS One. 7 (2012), https://doi.org/10.1371/journal.pone.0042754.
[114] T. Yamashita, S. Sonoda, R. Suzuki, N. Arimura, K. Tachibana, K. Maruyama, T. Sakamoto, A novel bubble liposome and ultrasound-mediated gene transfer to ocular surface: RC-1 cells *in vitro* and conjunctiva in vivo, Exp Eye Res. 85 (2007) 741–748, https://doi.org/10.1016/j.exer.2007.08.006.
[115] L. Kowalczuk, M. Boudinet, M. El Sanharawi, E. Touchard, M.-C. Naud, A. Saïed, J.-C. Jeanny, F. Behar-Cohen, P. Laugier, In vivo gene transfer into the ocular ciliary muscle mediated by ultrasound and microbubbles, Ultrasound Med Biol. 37 (2011) 1814–1827, https://doi.org/10.1016/j.ultrasmedbio.2011.07.010.
[116] H. Li, J. Qian, C. Yao, C. Wan, F. Li, Combined ultrasound-targeted microbubble destruction and polyethylenimine-mediated plasmid DNA delivery to the rat retina: enhanced efficiency and accelerated expression, J Gene Med. 18 (2016) 47–56, https://doi.org/10.1002/jgm.2875.
[117] C. Yan, D. Zhu, D. Huang, G. Xia, Role of ultrasound and microbubble-mediated heat shock protein 72 siRNA on ischemia-reperfusion liver injury in rat, Int J Clin Exp Med. 8 (2015) 5746–5752.
[118] Z.-Z. Jiang, G.-Y. Xia, Y. Zhang, L. Dong, B.-Z. He, J.-G. Sun, Attenuation of hepatic fibrosis through ultrasound-microbubble-mediated HGF gene transfer in rats, Clin Imaging. 37 (1) (2013) 104–110, https://doi.org/10.1016/j.clinimag.2012.02.017.
[119] Z.-X. Wang, Z.-G. Wang, H.-T. Ran, J.-L. Ren, Y. Zhang, Q. Li, Y.-F. Zhu, M. Ao, The treatment of liver fibrosis induced by hepatocyte growth factor-directed, ultrasound-targeted microbubble destruction in rats, Clin Imaging. 33 (6) (2009) 454–461, https://doi.org/10.1016/j.clinimag.2009.07.001.
[120] S.-H. Zhang, K.-M. Wen, W. Wu, W.-Y. Li, J.-N. Zhao, Efficacy of HGF carried by ultrasound microbubble-cationic nano-liposomes complex for treating hepatic fibrosis in a bile duct ligation rat model, and its relationship with the diffusion-weighted MRI parameters, Clin Res Hepatol Gastroenterol. 37 (6) (2013) 602–607, https://doi.org/10.1016/j.clinre.2013.05.011.
[121] Y.S. Li, E. Davidson, C.N. Reid, A.P. McHale, Optimising ultrasound-mediated gene transfer (sonoporation) *in vitro* and prolonged expression of a transgene in vivo: potential applications for gene therapy of cancer, Cancer Lett. 273 (2009) 62–69, https://doi.org/10.1016/j.canlet.2008.07.030.
[122] Y. Watanabe, S. Horie, Y. Funaki, Y. Kikuchi, H. Yamazaki, K. Ishii, S. Mori, G. Vassaux, T. Kodama, Delivery of Na/I symporter gene into skeletal muscle using nanobubbles and ultrasound: visualization of gene expression by PET, J Nucl Med. 51 (2010) 951–958, https://doi.org/10.2967/jnumed.109.074443.
[123] Y. Negishi, Y. Ishii, H. Shiono, S. Akiyama, S. Sekine, T. Kojima, S. Mayama, T. Kikuchi, N. Hamano, Y. Endo-Takahashi, R. Suzuki, K. Maruyama, Y. Aramaki, Bubble liposomes and ultrasound exposure improve localized morpholino oligomer delivery into the skeletal muscles of dystrophic mdx mice, Mol Pharm. 11 (3) (2014) 1053–1061, https://doi.org/10.1021/mp4004755.
[124] Y. Negishi, Y. Ishii, K. Nirasawa, E. Sasaki, Y. Endo-Takahashi, R. Suzuki, K. Maruyama, PMO Delivery System Using Bubble Liposomes and Ultrasound Exposure for Duchenne Muscular Dystrophy Treatment, Methods Mol Biol. 1687 (2018) 185–192, https://doi.org/10.1007/978-1-4939-7374-3_13.
[125] Y. Oishi, T. Kakimoto, W. Yuan, S. Kuno, H. Yamashita, T. Chiba, Fetal Gene Therapy for Ornithine Transcarbamylase Deficiency by Intrahepatic Plasmid DNA-Micro-Bubble Injection Combined with Hepatic Ultrasound Insonation, Ultrasound Med Biol. 42 (6) (2016) 1357–1361, https://doi.org/10.1016/j.ultrasmedbio.2015.10.007.
[126] Z. Song, Y. Ye, Z. Zhang, J. Shen, Z. Hu, Z. Wang, J. Zheng, Noninvasive, targeted gene therapy for acute spinal cord injury using LIFU-mediated BDNF-loaded cationic nanobubble destruction, Biochem Biophys Res Commun. 496 (3) (2018) 911–920, https://doi.org/10.1016/j.bbrc.2018.01.123.
[127] C.-Y. Lin, C.-H. Tsai, L.-Y. Feng, W.-Y. Chai, C.-J. Lin, C.-Y. Huang, K.-C. Wei, C.-K. Yeh, C.-M. Chen, H.-L. Liu, Focused ultrasound-induced blood brain-barrier opening enhanced vascular permeability for GDNF delivery in Huntington's disease mouse model, Brain Stimul. 12 (5) (2019) 1143–1150, https://doi.org/10.1016/j.brs.2019.04.011.
[128] P.-H. Hsu, K.-C. Wei, C.-Y. Huang, C.-J. Wen, T.-C. Yen, C.-L. Liu, Y.-T. Lin, J.-C. Chen, C.-R. Shen, H.-L. Liu, Noninvasive and targeted gene delivery into the brain using microbubble-facilitated focused ultrasound, PLoS One. 8 (2013), https://doi.org/10.1371/journal.pone.0057682 e57682.
[129] C.-H. Fan, C.-Y. Ting, C.-Y. Lin, H.-L. Chan, Y.-C. Chang, Y.-Y. Chen, H.-L. Liu, C.-K. Yeh, Noninvasive, Targeted, and Non-Viral Ultrasound-Mediated GDNF-Plasmid Delivery for Treatment of Parkinson's Disease, Sci Rep. 6 (2016) 19579, https://doi.org/10.1038/srep19579.
[130] P. Yue, L. Gao, X. Wang, X. Ding, J. Teng, Ultrasound-triggered effects of the microbubbles coupled to GDNF- and Nurr1-loaded PEGylated liposomes in a rat model of Parkinson's disease, J Cell Biochem. 119 (6) (2018) 4581–4591, https://doi.org/10.1002/jcb.v119.610.1002/jcb.26608.
[131] M. Decressac, N. Volakakis, A. Björklund, T. Perlmann, NURR1 in Parkinson disease—from pathogenesis to therapeutic potential, Nature Reviews, Neurology. 9 (11) (2013) 629–636, https://doi.org/10.1038/nrneurol.2013.209.

[132] S. Sonoda, K. Tachibana, E. Uchino, A. Okubo, M. Yamamoto, K. Sakoda, T. Hisatomi, K.-H. Sonoda, Y. Negishi, Y. Izumi, S. Takao, T. Sakamoto, Gene transfer to corneal epithelium and keratocytes mediated by ultrasound with microbubbles, Invest Ophthalmol Vis Sci. 47 (2006) 558–564, https://doi.org/10.1167/iovs.05-0889.
[133] Y. Sakakima, S. Hayashi, Y. Yagi, A. Hayakawa, K. Tachibana, A. Nakao, Gene therapy for hepatocellular carcinoma using sonoporation enhanced by contrast agents, Cancer Gene Ther. 12 (11) (2005) 884–889, https://doi.org/10.1038/sj.cgt.7700850.
[134] O. Zolochevska, X. Xia, B.J. Williams, A. Ramsay, S. Li, M.L. Figueiredo, Sonoporation delivery of interleukin-27 gene therapy efficiently reduces prostate tumor cell growth in vivo, Hum Gene Ther. 22 (12) (2011) 1537–1550, https://doi.org/10.1089/hum.2011.076.
[135] R. Suzuki, E. Namai, Y. Oda, N. Nishiie, S. Otake, R. Koshima, K. Hirata, Y. Taira, N. Utoguchi, Y. Negishi, S. Nakagawa, K. Maruyama, Cancer gene therapy by IL-12 gene delivery using liposomal bubbles and tumoral ultrasound exposure, J Control Release. 142 (2) (2010) 245–250, https://doi.org/10.1016/j.jconrel.2009.10.027.
[136] P. Hauff, S. Seemann, R. Reszka, M. Schultze-Mosgau, M. Reinhardt, T. Buzasi, T. Plath, S. Rosewicz, M. Schirner, Evaluation of gas-filled microparticles and sonoporation as gene delivery system: feasibility study in rodent tumor models, Radiology. 236 (2005) 572–578, https://doi.org/10.1148/radiol.2362040870.
[137] S. Zhou, S. Li, Z. Liu, Y. Tang, Z. Wang, J. Gong, C. Liu, Ultrasound-targeted microbubble destruction mediated herpes simplex virus-thymidine kinase gene treats hepatoma in mice, J Exp Clin Cancer Res. 29 (2010) 170, https://doi.org/10.1186/1756-9966-29-170.
[138] F. Nie, H.-X. Xu, M.-D. Lu, Y. Wang, Q. Tang, Anti-angiogenic gene therapy for hepatocellular carcinoma mediated by microbubble-enhanced ultrasound exposure: an in vivo experimental study, J Drug Target. 16 (5) (2008) 389–395, https://doi.org/10.1080/10611860802088846.
[139] X. Yu, S.-K. Song, J. Chen, M.J. Scott, R.J. Fuhrhop, C.S. Hall, P.J. Gaffney, S.A. Wickline, G.M. Lanza, High-resolution MRI characterization of human thrombus using a novel fibrin-targeted paramagnetic nanoparticle contrast agent, Magn Reson Med. 44 (6) (2000) 867–872, https://doi.org/10.1002/(ISSN)1522-259410.1002/1522-2594(200012)44:6<>1.0.CO;2-610.1002/1522-2594(200012)44:6<867::AID-MRM7>3.0.CO;2-P.
[140] W. Dong, P. Wu, M. Qin, S. Guo, H. Liu, X. Yang, W. He, A. Bouakaz, M. Wan, Y. Zong, Multipotent miRNA Sponge-Loaded Magnetic Nanodroplets with Ultrasound/Magnet-Assisted Delivery for Hepatocellular Carcinoma Therapy, Mol Pharm. 17 (8) (2020) 2891–2910, https://doi.org/10.1021/acs.molpharmaceut.0c0033610.1021/acs.molpharmaceut.0c00336.s001.
[141] H. Guo, M. Xu, Z. Cao, W. Li, L. Chen, X. Xie, W. Wang, J. Liu, Ultrasound-Assisted miR-122-Loaded Polymeric Nanodroplets for Hepatocellular Carcinoma Gene Therapy, Mol Pharm. 17 (2020) 541–553, https://doi.org/10.1021/acs.molpharmaceut.9b00983.
[142] X. Xie, Y. Yang, W. Lin, H. Liu, H. Liu, Y. Yang, Y. Chen, X. Fu, J. Deng, Cell-penetrating peptide-siRNA conjugate loaded YSA-modified nanobubbles for ultrasound triggered siRNA delivery, Colloids Surf B Biointerfaces. 136 (2015) 641–650, https://doi.org/10.1016/j.colsurfb.2015.10.004.
[143] W. Cai, W. Lv, Y. Feng, H. Yang, Y. Zhang, G. Yang, Y. Duan, J. Wang, The therapeutic effect in gliomas of nanobubbles carrying siRNA combined with ultrasound-targeted destruction, Int J Nanomedicine. 13 (2018) 6791–6807, https://doi.org/10.2147/IJN.S164760.
[144] Y. He, Y. Bi, X.-J. Ji, G. Wei, Increased efficiency of testicular tumor chemotherapy by ultrasound microbubble-mediated targeted transfection of siMDR1, Oncol Rep. 34 (2015) 2311–2318, https://doi.org/10.3892/or.2015.4262.
[145] M. Bai, M. Shen, Y. Teng, Y. Sun, F. Li, X. Zhang, Y. Xu, Y. Duan, L. Du, Enhanced therapeutic effect of Adriamycin on multidrug resistant breast cancer by the ABCG2-siRNA loaded polymeric nanoparticles assisted with ultrasound, Oncotarget. 6 (2015) 43779–43790. 10.18632/oncotarget.6085.
[146] S. Mullick Chowdhury, T.-Y. Wang, S. Bachawal, R. Devulapally, J.W. Choe, L. Abou Elkacem, B.K. Yakub, D.S. Wang, L.u. Tian, R. Paulmurugan, J.K. Willmann, Ultrasound-guided therapeutic modulation of hepatocellular carcinoma using complementary microRNAs, J Control Release. 238 (2016) 272–280, https://doi.org/10.1016/j.jconrel.2016.08.005.
[147] M. Wu, H. Zhao, L. Guo, Y. Wang, J. Song, X. Zhao, C. Li, L. Hao, D. Wang, J. Tang, Ultrasound-mediated nanobubble destruction (UMND) facilitates the delivery of A10–3.2 aptamer targeted and siRNA-loaded cationic nanobubbles for therapy of prostate cancer, Drug Deliv. 25 (1) (2018) 226–240, https://doi.org/10.1080/10717544.2017.1422300.
[148] K. Un, S. Kawakami, R. Suzuki, K. Maruyama, F. Yamashita, M. Hashida, Development of an ultrasound-responsive and mannose-modified gene carrier for DNA vaccine therapy, Biomaterials. 31 (30) (2010) 7813–7826, https://doi.org/10.1016/j.biomaterials.2010.06.058.
[149] K. Un, S. Kawakami, R. Suzuki, K. Maruyama, F. Yamashita, M. Hashida, Suppression of melanoma growth and metastasis by DNA vaccination using an ultrasound-responsive and mannose-modified gene carrier, Mol Pharm. 8 (2) (2011) 543–554, https://doi.org/10.1021/mp100369n.
[150] J.L. Tlaxca, J.J. Rychak, P.B. Ernst, P.R. Konkalmatt, T.I. Shevchenko, T.T. Pizarro, T.T. Pizzaro, J. Rivera-Nieves, A.L. Klibanov, M.B. Lawrence, Ultrasound-based molecular imaging and specific gene delivery to mesenteric vasculature by endothelial adhesion molecule targeted microbubbles in a mouse model of Crohn's disease, J Control Release. 165 (2013) 216–225, https://doi.org/10.1016/j.jconrel.2012.10.021.
[151] J.M. Orian, C.S. D'Souza, P. Kocovski, G. Krippner, M.W. Hale, X. Wang, K. Peter, Platelets in Multiple Sclerosis: Early and Central Mediators of Inflammation and Neurodegeneration and Attractive Targets for Molecular Imaging and Site-Directed Therapy, Frontiers in Immunology. 12 (2021) 349, https://doi.org/10.3389/fimmu.2021.620963.
[152] P. Roy, M. Orecchioni, K. Ley, How the immune system shapes atherosclerosis: roles of innate and adaptive immunity, Nat Rev Immunol. (2021) 1–15, https://doi.org/10.1038/s41577-021-00584-1.
[153] The top 10 causes of death, (n.d.). https://www.who.int/news-room/fact-sheets/detail/the-top-10-causes-of-death (accessed May 26, 2021).
[154] Z. Wang, S. Jiang, S. Li, W. Yu, J. Chen, D. Yu, C. Zhao, Y. Li, K. Kang, R. Wang, M. Liang, M. Xu, Y. Ou, P. Li, X. Leng, J. Tian, T. R-Porter, Targeted galectin-7 inhibition with ultrasound microbubble targeted gene therapy as a sole therapy to prevent acute rejection following heart transplantation in a Rodent model, Biomaterials. 263 (2020) 120366. 10.1016/j.biomaterials.2020.120366.
[155] Li Zhang, Zhenxing Sun, Pingping Ren, Manjie You, Jing Zhang, Lingyun Fang, Jing Wang, Yihan Chen, Fei Yan, Hairong Zheng, Mingxing Xie, Localized Delivery of shRNA against PHD2 Protects the Heart from Acute Myocardial Infarction through Ultrasound-Targeted Cationic Microbubble Destruction, Theranostics. 7 (1) (2017) 51–66, https://doi.org/10.7150/thno.16074.
[156] Wang Zhigang, Ling Zhiyu, Ran Haitao, Ren Hong, Zhang Qunxia, Huang Ailong, Liu Qi, Zhao Chunjing, Tang Hailin, Gong Lin, Peng Mingli, Pu Shiyu, Ultrasound-mediated microbubble destruction enhances VEGF gene delivery to the infarcted myocardium in rats, Clin Imaging. 28 (6) (2004) 395–398, https://doi.org/10.1016/j.clinimag.2004.04.003.
[157] Hiroko Fujii, Zhuo Sun, Shu-Hong Li, Jun Wu, Shafie Fazel, Richard D. Weisel, Harry Rakowski, Jonathan Lindner, Ren-Ke Li, Ultrasound-targeted gene delivery induces angiogenesis after a myocardial infarction in mice, JACC Cardiovasc Imaging. 2 (7) (2009) 869–879, https://doi.org/10.1016/j.jcmg.2009.04.008.
[158] H. Fujii, S.-H. Li, J. Wu, Y. Miyagi, T.M. Yau, H. Rakowski, K. Egashira, J. Guo, R. D. Weisel, R.-K. Li, Repeated and targeted transfer of angiogenic plasmids into the infarcted rat heart via ultrasound targeted microbubble destruction enhances cardiac repair, Eur Heart J. 32 (2011) 2075–2084, https://doi.org/10.1093/eurheartj/ehq475.
[159] Q. Zhou, Q. Deng, B. Hu, Y.-J. Wang, J.-L. Chen, J.-J. Cui, S. Cao, H.-N. Song, Ultrasound combined with targeted cationic microbubble-mediated angiogenesis gene transfection improves ischemic heart function, Exp Ther Med. 13 (2017) 2293–2303, https://doi.org/10.3892/etm.2017.4270.
[160] M. Ziegler, J.D. Hohmann, A.K. Searle, M.-K. Abraham, H.H. Nandurkar, X. Wang, K. Peter, A single-chain antibody-CD39 fusion protein targeting activated platelets protects from cardiac ischaemia/reperfusion injury, Eur Heart J. 39 (2018) 111–116, https://doi.org/10.1093/eurheartj/ehx218.
[161] Laura A. Bienvenu, Ana Maluenda, James D. McFadyen, Amy K. Searle, Eefang Yu, Carolyn Haller, Elliot L. Chaikof, Karlheinz Peter, Xiaowei Wang, Combined Antiplatelet/Anticoagulant Drug for Cardiac Ischemia/Reperfusion Injury, Circulation Research. 127 (9) (2020) 1211–1213, https://doi.org/10.1161/CIRCRESAHA.120.317450.
[162] Xia He, Da-Fang Wu, Jun Ji, Wen-ping Ling, Xiao-ling Chen, Yue-Xuan Chen, Ultrasound microbubble-carried PNA targeting to c-myc mRNA inhibits the proliferation of rabbit iliac arterious smooth muscle cells and intimal hyperplasia, Drug Deliv. 23 (7) (2016) 2482–2487, https://doi.org/10.3109/10717544.2015.1014947.
[163] Wei J. Cao, Joshua D. Rosenblat, Nathan C. Roth, Michael A. Kuliszewski, Pratiek N. Matkar, Dmitriy Rudenko, Christine Liao, Paul J.H. Lee, Howard Leong-Poi, Therapeutic Angiogenesis by Ultrasound-Mediated MicroRNA-126-3p Delivery, Arterioscler Thromb Vasc Biol. 35 (11) (2015) 2401–2411, https://doi.org/10.1161/ATVBAHA.115.306506.
[164] Y. Endo-Takahashi, Y. Negishi, A. Nakamura, S. Ukai, K. Ooaku, Y. Oda, K. Sugimoto, F. Moriyasu, N. Takagi, R. Suzuki, K. Maruyama, Y. Aramaki, Systemic delivery of miR-126 by miRNA-loaded Bubble liposomes for the treatment of hindlimb ischemia, Sci Rep. 4 (2014) 3883, https://doi.org/10.1038/srep03883.
[165] Danny M. Skyba, Richard J. Price, Andre Z. Linka, Thomas C. Skalak, Sanjiv Kaul, Direct in vivo visualization of intravascular destruction of microbubbles by ultrasound and its local effects on tissue, Circulation. 98 (4) (1998) 290–293, https://doi.org/10.1161/01.CIR.98.4.290.
[166] D.L. Miller, J. Quddus, Diagnostic ultrasound activation of contrast agent gas bodies induces capillary rupture in mice, Proc Natl Acad Sci U S A. 97 (18) (2000) 10179–10184, https://doi.org/10.1073/pnas.180294397.
[167] T. Ay, X. Havaux, G. Van Camp, B. Campanelli, G. Gisellu, A. Pasquet, J.F. Denef, J.A. Melin, J.L. Vanoverschelde, Destruction of contrast microbubbles by ultrasound: effects on myocardial function, coronary perfusion pressure, and microvascular integrity, Circulation. 104 (2001) 461–466, https://doi.org/10.1161/hc3001.092038.
[168] J.F. Zachary, S.A. Hartleben, L.A. Frizzell, W.D. O'Brien, Arrhythmias in rat hearts exposed to pulsed ultrasound after intravenous injection of a contrast agent, J Ultrasound Med. 21 (2002) 1347–1356; discussion 1343-1345. 10.7863/jum.2002.21.12.1347.
[169] Douglas L. Miller, Peng Li, Chunyan Dou, David Gordon, Chris A. Edwards, William F. Armstrong, Influence of contrast agent dose and ultrasound exposure on cardiomyocyte injury induced by myocardial contrast echocardiography in rats, Radiology. 237 (1) (2005) 137–143, https://doi.org/10.1148/radiol.2371041467.

[170] Douglas L. Miller, Edward M. Driscoll, Chunyan Dou, William F. Armstrong, Benedict R. Lucchesi, Microvascular permeabilization and cardiomyocyte injury provoked by myocardial contrast echocardiography in a canine model, J Am Coll Cardiol. 47 (7) (2006) 1464–1468, https://doi.org/10.1016/j.jacc.2005.09.078.

[171] Bart Geers, Ine Lentacker, Angelika Alonso, Niek N. Sanders, Joseph Demeester, Stephen Meairs, Stefaan C. De Smedt, Elucidating the mechanisms behind sonoporation with adeno-associated virus-loaded microbubbles, Mol Pharm. 8 (6) (2011) 2244–2251, https://doi.org/10.1021/mp200112y.

[172] Yoichi Negishi, Yuka Tsunoda, Nobuhito Hamano, Daiki Omata, Yoko Endo-Takahashi, Ryo Suzuki, Kazuo Maruyama, Motoyoshi Nomizu, Yukihiko Aramaki, Ultrasound-mediated gene delivery systems by AG73-modified Bubble liposomes, Biopolymers. 100 (4) (2013) 402–407, https://doi.org/10.1002/bip.22246.

[173] H. Dewitte, K. Vanderperren, H. Haers, E. Stock, L. Duchateau, M. Hesta, J.H. Saunders, S.C. De Smedt, I. Lentacker, Theranostic mRNA-loaded microbubbles in the lymphatics of dogs: implications for drug delivery, Theranostics. 5 (2015) 97–109, https://doi.org/10.7150/thno.10298.

[174] B.-F. Yu, J. Wu, Y. Zhang, H.-W. Sung, J. Xie, R.-K. Li, Ultrasound-targeted HSVtk and Timp3 gene delivery for synergistically enhanced antitumor effects in hepatoma, Cancer Gene Ther. 20 (5) (2013) 290–297, https://doi.org/10.1038/cgt.2013.19.

[175] Hongbo Li, Ziyu Wang, Jia Zhang, Chenyan Yuan, Hao Zhang, Xinxin Hou, Dongsheng Zhang, Carlos Gómez, Severin P. Schwarzacher, Enhanced shRNA delivery by the combination of polyethylenimine, ultrasound, and nanobubbles in liver cancer, Technol Health Care. 27 (2019) 263–272, https://doi.org/10.3233/THC-199025.